Adsorption
https://doi.org/10.1007/s10450-024-00519-x

Development of biodegradable gum guggul-based hydrogel as an efficient moisture-retaining agent for agricultural applications

Shabnum Saleem[1] · Kashma Sharma[2] · Amit Kumar Sharma[3,4] · Vishal Sharma[5] · Vaneet Kumar[1] · Vijay Kumar[6]

Received: 30 April 2024 / Revised: 3 July 2024 / Accepted: 4 July 2024

Abstract

We prepared guggul gum-based hydrogel (GgG-cl-poly(AA)) through a free radical graft copolymerization mechanism in this work. The preparation was carried out using ammonium persulfate as an initiator, acrylic acid as the monomer, and N, N′-methylenebisacrylamide as the crosslinker. The synthesized hydrogel's swelling capacity and equilibrium swelling ratio were thoroughly investigated by optimizing various reaction parameters: reaction time, solvent volume, microwave power, crosslinker amount, initiator concentration, and monomer concentration. The swelling results demonstrated that the synthesized hydrogel can attain a maximum percentage swelling of 980% within 3 h in an aqueous solution. The prepared hydrogel sample was characterized using Fourier transform infrared, X-ray diffraction, scanning electron microscopy, nuclear magnetic resonance, and thermogravimetric analysis. The prepared hydrogel was studied for water retention behavior in the soil, water absorbance in the open air at room temperature, reswelling studies, and resistive swelling studies in various salt solutions at different temperatures and pH values. Notably, the crosslinked hydrogel exhibited a reduced swelling capacity across various salt solutions compared to the aqueous solutions. The biodegradation studies were examined in both soil burial and vermicomposting methods for two months, revealing a maximum biodegradation of 95.65% through the vermicomposting method and 87.7% through the soil burial method. The results indicate that the crosslinked hydrogel based on guggul gum is a potential candidate for various agricultural applications.

Keywords Hydrogel · Biodegradation · Crosslinker · Water retention · Vermicompost

1 Introduction

In the current scenario, sustainable development in agriculture and forestry is a prime objective worldwide [1–3]. However, the sustainability of the agriculture and forestry sectors is threatened by many factors, such as water scarcity, droughts, and soil degradation [4]. The absence of rainfall and irrigation water poses a critical challenge in arid and semiarid regions, where water is pivotal for enhancing crop yield and cultivable land [5]. Additionally, sandy soils exhibit low water-holding capacities, leading to substantial runoff of rain and irrigation water beyond the root zone, resulting in ineffective fertilizer and water utilization. Conversely, clay soils suffer from inadequate ventilation and a compact structure [6–8]. Water stress conditions arise from various factors, including insufficient soil water retention, nutrient and water seepage into deeper layers, and excessive surface runoff. The agricultural domain is acutely susceptible to drought stress, posing a substantial threat to global food security [9]. Globally, 70% of fresh water is allocated

✉ Vijay Kumar
vj.physics@gmail.com

[1] Department of Environmental Science, CT University, Ferozepur Road, Sidhwan Khurd, Punjab 142024, India

[2] Department of Chemistry, DAV College, Sector-10, Chandigarh 160011, India

[3] Department of Chemistry, University Institute of Sciences, Chandigarh University, Mohali, Punjab 140413, India

[4] University Centre for Research and Development, Chandigarh University, Mohali, Punjab 140413, India

[5] Institute of Forensic Science & Criminology, Panjab University, Chandigarh 160014, India

[6] Department of Physics, National Institute of Technology Srinagar, Srinagar, Jammu and Kashmir 190006, India

Published online: 28 July 2024

for agricultural use. By 2050, an estimated 50% increase in farm output and a 15% surge in water withdrawals will be indispensable to sustain a planet inhabited by nine billion people [10]. Traditionally, direct plant watering has been the cornerstone of agricultural management. While this technique remains prevalent, alternative management approaches like flood (furrow), drip irrigation, and spray irrigation have also proven effective and efficient [11].

Nevertheless, conventional irrigation methods do not facilitate complete water absorption by plants; a fraction of water evaporates, and others seep deep into the soil. Given the precarious water situation, enhanced water management is urgently necessary to maintain a readily available water supply in the soil surrounding plant roots [12]. The latest water-saving deficit irrigation technologies are pivotal for achieving a favorable soil moisture balance in the root zone, promising higher water use efficiency without embarrassing crop production and quality [13, 14]. Contemporary advancements in irrigation technologies, such as low-pressure micro sprinklers and drip irrigation systems coupled with plastic mulching, can ease water scarcity by significantly reducing irrigation water consumption [9, 15, 16]. However, these high-tech tools are predominantly utilized in high-value crops and entail substantial capital, ongoing operational costs, and specialized knowledge requirements for farmers. Another viable solution is exploring alternative irrigation technologies that employ highly expandable superabsorbent hydrogels (SAHs) to alleviate soil moisture stress and enhance production [17]. Many countries rely heavily on virtual water supplies in arid regions for their daily needs. Over time, adopting cutting-edge technologies to improve nutrient and water utilization efficiency may become increasingly critical, particularly in areas with limited water resources.

In agriculture, SAHs are essential for promoting environment-friendly conditions and improving water irrigation efficiency [18]. They can serve as reservoirs to prevent water waste and enhance irrigation efficiency by absorbing and retaining water several times their initial dry weight. Additionally, SAHs can improve the specific physical properties of the soil [19]. Hydrogels are 3D crosslinked networks of hydrophilic polymers capable of absorbing and swelling in water [20], exhibiting numerous exceptional properties, and finding substantial properties including high water permeability for metabolites, hydrophilicity, resistance to oxygen, tissue-mimicking consistency, and environmental responsiveness [21]. Hydrogels are applied in diverse fields, including agricultural, industrial, biomedicine, wastewater treatment [22], designing contact lenses, tissue engineering [23], sustained drug delivery [24, 25], and wound healing [26]. Among various hydrogels, the environmentally-sensitive hydrogels are the most prominent class, and globally, they draw significant interest from researchers [27]. SAHs appear exceptionally beneficial in agriculture as soil conditioners for enhancing crop growth in sandy or clayey soils. SAHs are widely employed as soil conditioners for improving crop productivity and reducing soil water loss [28]. For agricultural applications, the hydrogels must exhibit desirable properties such as nontoxicity, non-disruptiveness to the soil nutrients, stability in the soil, and, crucially, cost-effectiveness [29, 30]. Microwave synthesis is often called a green synthesis approach due to its minimal waste production and rapid generation of free radicals from the initiator, which facilitates the formation of short-chain porous polymeric products. This process combines the effects of microwaves and heating [31, 32].

Guggul is an oleo-gum resin of 2–8% volatile oil, 23–40% resin fraction, 40–60% gum fraction, and 10–25% bitter principle [33]. *Commiphora Mukul (Guggul)* exudes from the bark of the Mukul myrrh tree and is found in Pakistan, Somalia, and India. Complete hydrolysis of highly branched polysaccharides yields components such as L-arabinose, D-galactose, L-fucose, 4-O-methyl-Dglucoronic acid, and aldobiouronic acid [33, 34]. Numerous studies, articles, brief communications, and monographs have been written about the usage of hydrogels for agricultural purposes. Ahmad et al. [35] used a simple method to synthesize superabsorbent hydrogels using polyvinyl alcohol crosslinked with borax and Moringa oléifera gum. The prepared hydrogel showed good density, water retention ability, swelling ratio, salt sensitivity, and reswelling properties. Liu et al. [4] synthesized fenugreek galactomannan-borax-based hydrogel for agricultural purposes. They mixed the hydrogel with the soil to analyze the soil's ability to absorb water, which was assessed as a latent water retention agent. This cost-effective and environmentally friendly hydrogel has many potential agricultural uses for preserving soil water. Meng et al. [36] utilized hydrogels prepared from acrylic acid (AA) and the waste obtained from the industrial sector. They exhibited super-swelling and slow-release behavior in water, making them excellent candidates for water retention agents in agriculture. The primary objective of this work was to present a new and simple technique for creating super-swelling biopolymeric hydrogels with long-term water retention qualities using polysaccharides and lignosulphonate, the primary ingredients in red liquor. Abdallah [37] revealed the effects of hydrogel particle size on the amount of water preserved by the hydrogel, the amount of water used each day, and the survival of guava seedlings under drought-like conditions. Another goal of this study was to examine how hydrogel's particle size impacts the soil's physical characteristics, such as AWC, WHC, and saturated hydraulic conductivity. Patra et al. [38] reported that when hydrogel is added to soil, it hydrates to create an amorphous gelatinous material and can

adsorb and desorb water cyclically over an extended period. They determine the effectiveness of hydrogel on soil water retention and release properties for reducing drought stress and enhancing crop production under moisture-stress circumstances. Iftime and associates [39] examined new soil conditioner techniques for soil fertilization and water retention. These techniques were prepared *via* the in situ hydrogelation of chitosan with salicylaldehyde in the presence of fertilizer. These studies identified the novel systems as innovative, multifunctional, and eco-products that can address problems related to soil conditioning and water retention.

Guggul gum-based materials have been explored for various industrial and medical applications; however, as per our literature survey, no research paper regarding their use in the agricultural sector is available. A quick and effective method has been developed to create GgG-based hydrogel, which is aqueous-based, catalyst-free, inexpensive, environment friendly, and may find use in agriculture [35, 40]. Here, we described the role of *Guggul* gum-based hydrogel in the agriculture field, specifically for examining its swelling capacity, water retention properties in soil and the open air, biodegradability, salt-resistive swelling study at different temperatures and pH levels, and reswelling properties to evaluate its promising applications towards sustainable agriculture.

2 Materials and methods

2.1 Materials

Guggul gum (GgG) was purchased from the local market in Chandigarh, India. Acrylic acid (AA) and *N*, *N*-'methylenebisacrylamide (MBA) were purchased from Merck, Germany. Ammonium persulfate (APS) was obtained from Sigma Aldrich. Vermicompost was purchased from an agricultural shop on Court Road, Srinagar, India, while garden soil was collected from NIT Gardens in Srinagar, India. Distilled water was used for all synthesis procedures.

2.2 Purification of backbone

Guggul gum was extracted from a plant known as *Commiphora wightii* or *Commiphara Mukul*. The purification process of *guggul* gum was carried out in two steps. The first step involves manually removing exterior contaminants such as dry leaves and other foreign objects and breaking them into small pieces. In the second step, these pieces were dissolved in distilled water and placed in a glass beaker over a hot plate at 60 °C. The mixture was stirred until a fine slurry was formed. It was further filtered through a muslin cloth. A significant amount of ethanol was added to the slurry, and the purified gum obtained was allowed to dry in a hot air oven at 60 °C overnight. A fine powder of gum was made with the help of a pestle and mortar [41].

2.3 Synthesis of hydrogel

The superabsorbent GgG hydrogel was fabricated by a free radical polymerization using APS as an initiator, AA as a monomer, and MBA as a cross-linker. A desirable amount of GgG was uniformly dispersed in 11 mL of distilled water. A predetermined quantity of MBA, AA, and APS were mixed in the same beaker according to the desired ratios. The mixture was stirred and subjected to microwave irradiation for 60 s. The developed hydrogel was then placed in a hot air oven and dried at 60 °C overnight, as shown in Scheme 1.

2.4 Swelling studies

The swelling studies of the prepared hydrogels were determined by the pre-existing method [41]. Initially, the dried hydrogel was weighed over the weighing balance, kept in distilled water, and permitted to reach swelling equilibrium at room temperature. The swollen hydrogels were taken out and weighed at certain intervals after blotting the surface water with tissue paper. This process continued till the achievement of the equilibrium swelling percentage. Afterward, the swelling capacity (SC) was calculated using Eq. 1.

$$SC\% = \frac{W_e - W_d}{W_d} \times 100 \quad (1)$$

Where SC represents the swelling capacity of synthesized hydrogel, W_e are the weight of the equilibrium-swollen hydrogel, and W_d is the initial weight of the dried hydrogel.

After optimizing various reaction parameters to form a crosslinked network, the replications were carried out in triplicates. The reproducibility and statistical analysis of the results was carried out using the Statistical Package for Social Science (SPSS) version 10.

2.5 Water retention study

This study aimed to assess how a natural hydrogel affected the water retention capabilities of various types of soils, including sandy soil, clayey soil, and a combination of the two soils. In the typical procedure, 1 g of each hydrogel sample was placed in plastic bottles with 100 g of each soil sample. The vessels were filled with 50 ml of tap water and gently weighed over an analytical balance (accuracy = 0.00001 g). A control sample of untreated soil was included in the experiment to ensure that no weight loss had

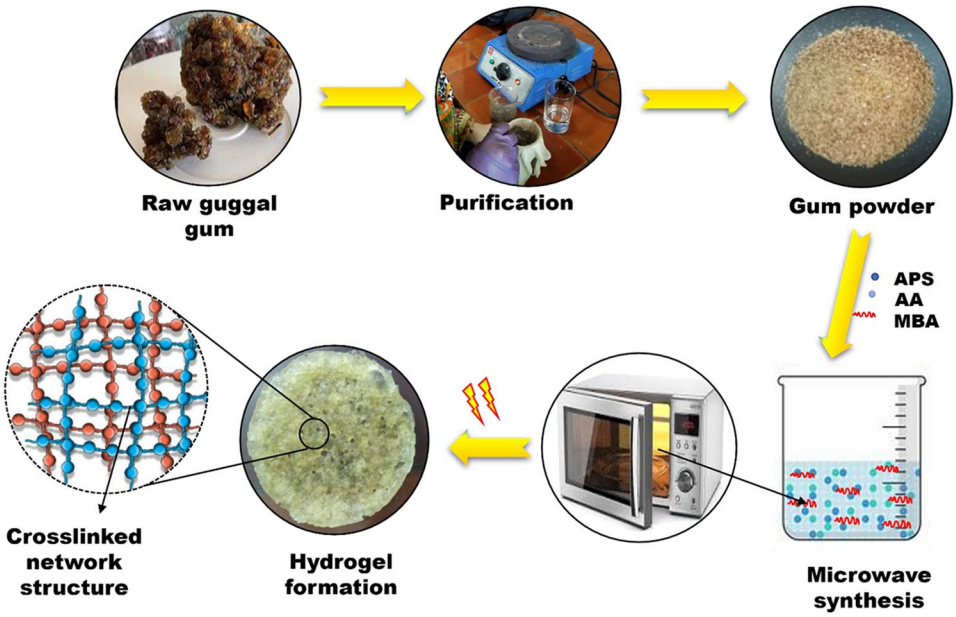

Scheme 1 Purification and synthesis of GgG-cl-poly(AA) hydrogel

occurred [42]. The vessels were kept at room temperature and weighed after regular intervals to determine the proportion of water retained by different types of soils. Equation 2 was used to calculate the water retention rate of the hydrogel.

$$WRR\% = \frac{S_i - S_f}{V} \times 100 \quad (2)$$

Where WRR% represents the water retention rate of the soil, S_i is the initial weight of the vessel, S_f is the final weight of the vessel, and V is the volume of the water used for maintaining the moisture level in the soil.

2.6 Water absorption study

The behavior of hydrogel in terms of water absorbance was examined using the gravimetric method. Dry samples were weighed as C_d and then submerged in excess water until they reached equilibrium at neutral pH and different temperatures (10 °C, 30 °C, and 60 °C). The swollen samples were removed, wiped off with tissue paper, and weighed as C_i. They were then dried in the open air at room temperature (relative humidity ≈ 50%). The samples were weighed at predetermined time intervals (C_t), and this process was repeated until the sample weight became constant [35, 40, 43]. Equation 3 was used to calculate the water absorption percentage.

$$WAR\% = \frac{C_t - C_d}{C_i - C_d} \times 100 \quad (3)$$

Where *WAR%* shows the water absorption percentage of the hydrogel, C_t represents the weight of the hydrogel after dehydration of the sample.

2.7 Salt resistive swelling study

This study examined the influence of ionic strength from different cations on the degree of swelling of the hydrogel in NaCl, $CaCl_2$, and $FeCl_3$ salt solutions at predefined time intervals and temperatures using distilled water. Salt solutions with different ionic strengths (0.01 M, 0.05 M, 0.1 M, 0.5 M) and cationic charge (monovalent, divalent, and trivalent) were prepared. 0.2 g of each dried hydrogel sample was immersed in different salt solutions of known proportions. After 3 h, the swollen gel was weighed, and $\%Q_t$ was calculated using Eq. 4 [42].

$$QT\% = \frac{W_t - M_o}{M_o} \times 100 \quad (4)$$

Where M_t and M_o are the weights of the samples in the swollen and dry states (in saline solutions), respectively, and Q_t is the qualitative time of salt resistive swelling percentage at a given time.

2.8 Temperature-responsive swelling

Different swelling ratios indicated that the hydrogel is temperature-sensitive. We took pre-weighed samples (0.2 g) and dipped them in distilled water at various temperatures (3°C, 25°C, 60°C, 80°C) using a refrigerator, room temperature, hot air oven, and vacuum oven. At regular intervals of

one hour, we removed the samples and weighed them until the hydrogel reached its equilibrium weight [42]. The swelling ratio was calculated using Eq. 1.

2.9 pH-responsive swelling

Buffer solutions with different pH values, ranging from 3.0 to 11, were used to evaluate the swelling behavior of GgG-cl-poly(AA) at various pH levels. Following established procedures outlined in the literature, we prepared alkaline and acidic solutions [42]. We employed a microprocessor pH meter (ATC) to measure the pH readings precisely. Known amounts of the dried hydrogel were submerged in various pH solutions, and the pH-responsive swelling percentage was calculated using Eq. 1.

2.10 Reswelling study

We employed distilled water to submerge a pre-weighted dry hydrogel sample (0.2 g) to confirm that it reached its swelling equilibrium and then re-weighted it. The swelled hydrogels were dried at 60 °C in a hot air oven for 12 h. After drying, the hydrogel sample was re-soaked in distilled water to calculate its equilibrium swelling capacity. We repeated this swelling and drying process five times using the same hydrogel sample. We also assessed the losses in the equilibrium swelling capacity of the same hydrogel sample [35].

2.11 Biodegradation studies

Biodegradation tests of GgG-cl-poly(AA) were conducted after the disposal of hydrogel samples in the soil, which involved soil burial and vermicomposting procedures. 0.5 g samples of GgG-cl-poly(AA) were taken and buried at a depth of 2 cm circularly with an equal distance of 3 cm in the pots containing garden soil and vermicompost. After specific intervals, one sample from each pot was removed, cleaned, dried, and precisely weighed. The biodegradation studies were conducted for 65 days. Instrumental methods such as FE-SEM and FTIR investigations were used to examine biodegradability qualitatively [32]. The percentage of biodegradation (BD%) was determined using Eq. 5.

$$BD\,\% = \frac{W_i - W_f}{W_i} \times\ 100 \tag{5}$$

Where W_i is the initial weight of the sample, and W_f is the final weight of the degraded sample.

2.12 Characterization

The characterization of gum *guggul* and GgG-cl-poly(AA) hydrogel was carried out using various instrumentation techniques. A microwave oven, IFB model-17PM-MEC1, was used with power requirements of 1200 W and a frequency of 2450 MHz. An FTIR spectrophotometer (PerkinElmer) equipped with ATR mode, diamond crystal, and ZnSe for the focusing component was used to record the FTIR spectra. The scan parameters were set between 4000–400 cm^{-1} with a resolution of 4 cm^{-1}. SEM Hitachi 3600 N scanning electron microscope with a 5-axis motorized stage and an ultra-dry compact EDS Detector (Thermo Scientific™) were used for high-resolution imaging and elemental analysis, respectively. X-ray studies were conducted on an X-ray Diffractometer operating at 40 kV and 30 mA with a Cu-K_β filter, scan range ($5^o<\theta<160^o$), and scan axis 2θ. TGA studies were performed on Perkin Elmer equipment to assess the material's thermal stability. The Bruker ^{1}H nuclear magnetic resonance cryomagnetic spectrophotometer (^{1}H NMR) at 400 MHz was used to determine its chemical structure precisely.

3 Results and discussion

3.1 Optimization and analysis of the maximum swelling percentage

The optimization and maximum SC of GgG-cl-poly(AA) hydrogel at various initiator concentrations ranging from 0.00796 to 0.01991×10^{-3} mol/L were investigated and presented in Fig. 1a. Initially, SC increased at 0.00796 mol/L initiator concentration and then decreased with a further increase in initiator concentration. The maximum swelling capacity (700%) was observed at 0.015918 mol/L of initiator concentration. The suggested trend was evident because the enhancement in initiator concentration can generate more free radicals, increasing grafting effectiveness and improving water absorption [44]. However, excessive initiator addition beyond the optimum value may terminate the free radical reaction prematurely and hinder the grafting yield [45]. Furthermore, increased reaction velocity and bimolecular collision favor the chain-terminating step when the initiator concentration exceeds an optimal level, depending on process parameters and reactant properties.

Consequently, a lower SC was observed at high initiator concentrations [44, 45]. The solvent amount also affected the swelling capacity of GgG-cl-poly(AA). Figure 1b illustrates that SC initially increased up to 710% at 11 mL of solvent volume and then decreased due to an optimal solvent concentration, which generates hydroxyl free radicals,

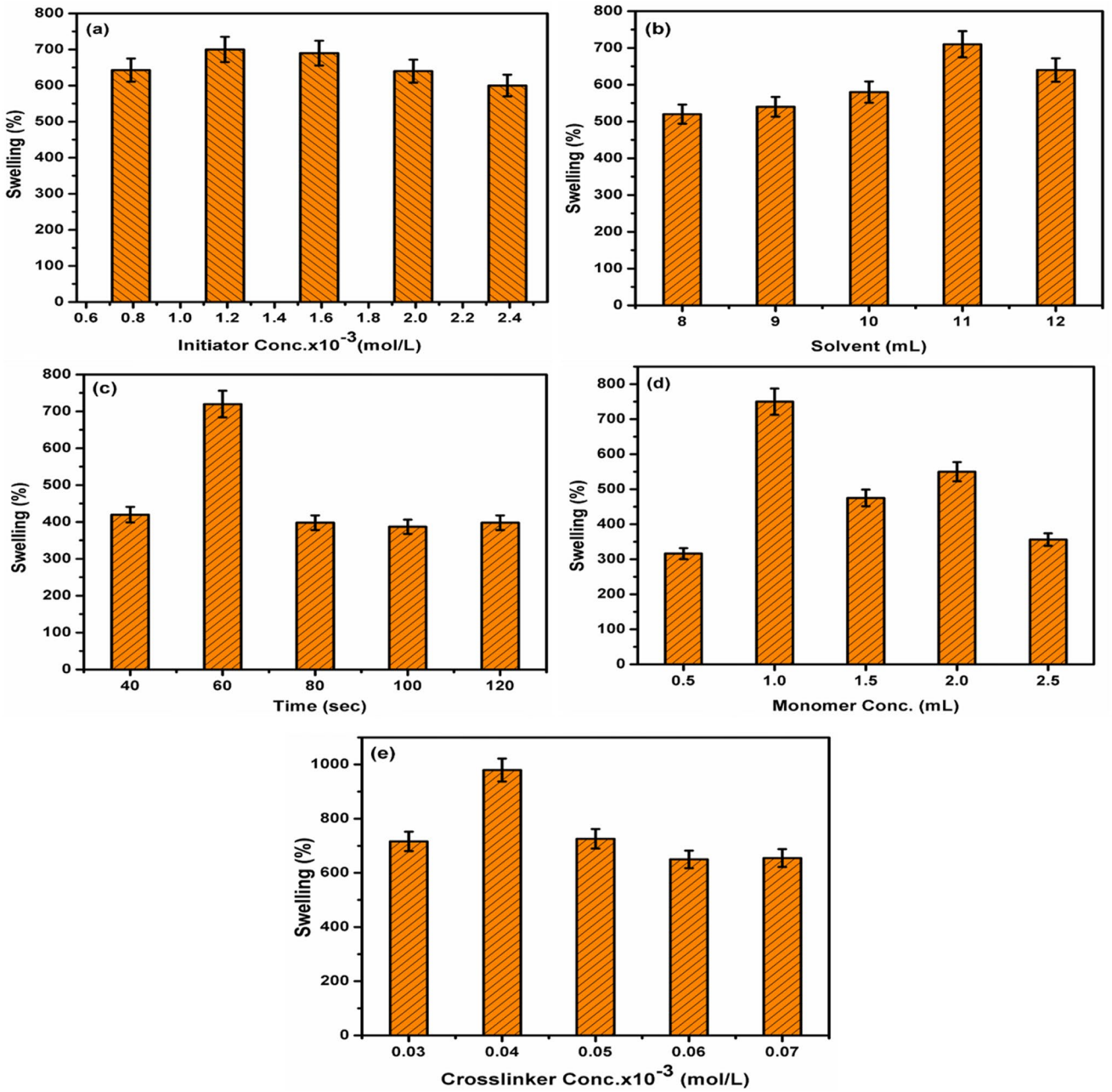

Fig. 1 Variation of percentage swelling with reaction parameters

creating more active sites for reaction propagation. Beyond this optimal level, an increase in solvent concentration causes a decline in SC because the GgG and AA have fewer active sites available for free radical graft polymerization [46]. Solvent concentration significantly affects the SC during the synthesis of crosslinked hydrogels. The energy obtained from microwave irradiation and absorbed by the solvent to produce hydroxyl free radicals contributes considerably to the dispersion of the copolymerization reaction, resulting in an initial rise in SC [45]. Figure 1c demonstrates that the optimized time was 60 s with a maximum swelling percentage of 720%. Initially, when the reaction time increased from 40 to 80 s, SC decreased, primarily due to the formation of shorter polymer chains that hindered the absorption of water molecules [45].

Conversely, prolonged reaction times led to increased crosslinking in the polymer, with multiple branched chains causing entanglement and forming small holes in three-dimensional networks, restricting polymer expansion. Hence, terse and long reaction times resulted in lower water absorbency [45]. Beyond 60 s, the additional free radicals attempted to stop the crosslinking process and increased the

Table 1 The optimized reaction parameters for synthesizing GgG-cl-poly(AA)

Sample code GGGG	Optimized reaction parameters										
	Back-bone (g)	Initiator concentration (mol/L) 10^{-3}	Solvent amount (mL)	Time (sec)	Monomer concentration (mL)	pH	Micro-wave Power (%)	Crosslinker concentration (mol/L) 10^{-3}	Mean percentage swelling (M)	±SD	±SE
GgG-cl-poly(AA)	0.5	0.0079	11	60	1	7	100	0.0079	980	26.76	15.45

Where no of replication = 3, M = mean, ±SD = standard deviation, and ± SE = standard error of the mean

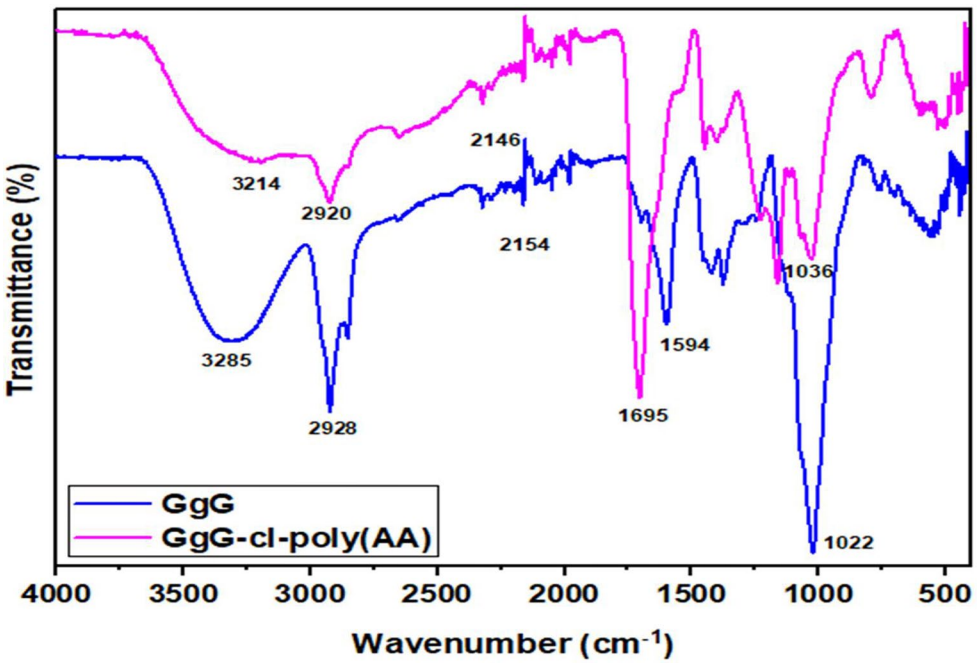

Fig. 2 FTIR spectra of (**a**) GgG and (**b**) GgG-cl-poly(AA)

possibility of adverse reactions such as homopolymerization [45]. Monomer concentration significantly affects the hydrogel's swelling capacity. The swelling behaviour of crosslinked hydrogel was investigated at various monomer concentrations ranging from 0.5 to 2.5 mL. Figure 1d shows the maximum swelling percentage obtained at 1 mL of AA concentration. Beyond this optimum value, the swelling percentage decreases with a further increase in monomer concentration. After optimization, the decrease in SC may be attributed to the reduction of active sites on the GgG backbone as graft copolymerization starts.

Additionally, excessive monomer concentration can lead to the formation of homopolymers or self-crosslinking networks, which thickens the reaction medium and hampers the movement of free radicals [47]. In addition, a decline in the osmotic pressure difference may cause the hydrogel network to contract [44–46]. The swelling capacity of polymer absorbent relies mainly on the polymer composition and properties of the external solution [46, 48]. It is widely recognized that adding excessive crosslinkers to the reaction mixture reduces the SC of hydrogel because the crosslinker molecules can settle between the polymer chains, which may reduce the availability of hydrophilic functional groups and decrease SC. Figure 1e shows the effect of MBA concentrations on the swelling capacity of GgG-cl-poly(AA). The optimized crosslinker concentration was 0.054×10^{-3} mol/L with an 847% maximum swelling capacity of the synthesized hydrogel [45, 49]. All the optimization experiments were performed three times, and the optimized concentration of each parameter is summarized in Table 1.

3.2 FTIR analysis

Figure 2 presents the FTIR spectra of guggul gum and GgG-cl-poly(AA) hydrogel. The FTIR spectrum of GgG exhibits a broad peak at 3285 cm^{-1} that may be attributed to OH stretching vibrations. The 2928 cm^{-1} peaks and 2154 cm^{-1} may correspond to N-H symmetric stretching vibrations. The FTIR data confirmed that GgG consists of protein moieties and polysaccharides and exhibits a broad transmittance associated with the O-H stretching of carbohydrates [45, 46]. The sharp peak obtained at 1022 cm^{-1} represents stretching and bending vibrations of C = O, C-C, C-H C-O-C, and C-O-H groups. The peak obtained at 1594 cm^{-1} indicates the presence of carboxylate groups of amino acids [47]. Upon crosslinking the GgG with AA, some changes

in the FTIR spectra have been observed. The disappearance of the O-H stretching peak and the appearance of two amide N-H symmetric stretching peaks at 3285 cm^{-1} and asymmetric stretching peaks at 3214 cm^{-1} clearly show the transformation of the backbone into a crosslinked hydrogel network [50, 51].

Further, the C-N stretching frequency at 1594 cm^{-1} is also visible in the IR spectrum of hydrogel, confirming the presence of acrylic acid [33]. A peak at 1695 cm^{-1} corresponding to C=O stretching vibrations confirmed the presence of acrylic acid in the synthesized hydrogel [41]. Compared to the backbone GgG, the presence of additional bands and a shift in the peak position confirmed the presence of AA chains in the synthesized hydrogel network [31].

3.3 X-ray diffraction studies

XRD patterns of GgG and GgG-cl-poly(AA) are shown in Fig. 3. The backbone GgG exhibited a broad peak at 20.22° on the 2θ scale, indicating its smooth and semi-crystalline structure. The main amorphous feature of GgG is designated by its low-intensity diffraction pattern [32, 49]. However, when the backbone was transformed into a crosslinked hydrogel network, its crystalline nature increased, with a slight peak position shift to 20.45° [45]. This shift occurs when a long-range ordered configuration is formed in the crosslinked hydrogel network, enhancing its crystalline nature [50]. When correctly positioned over the gum surface, the acrylic acid chain causes the system to transition to a more crystalline form with a few small and sharp peaks [35, 52]. Changes in peak broadening, sharpness, and position indicate the transformation of GgG into a more crystalline form following crosslinking, which was further validated by SEM analysis.

3.4 Surface morphological analysis

SEM findings of GgG and GgG-cl-poly(AA) demonstrated the morphological changes obtained after crosslinking the GgG surface with the AA moieties illustrated in Fig. 4. The smooth surface is depicted in the SEM image of GgG, indicating the homogeneous nature of the gum visible in Fig. 4a [47, 48]. After grafting with polyacrylic acid chains, the surface of GgG undergoes morphological alterations, distinguishing the crosslinked product from the backbone [31, 33]. Figure 4b shows the SEM investigations of synthesized hydrogel and reveals that the smooth surface of the backbone has been transformed into a rough and crosslinked structure, providing evidence of crosslinking [41].

3.5 Thermal analysis (TGA)

TGA provides information in a disciplined manner related to the changes occurring in the mass of material concerning time and temperature [50]. TGA was used to examine the thermal characteristics of GgG and GgG-cl-poly(AA), as shown in Fig. 5. In the GgG-cl-case of poly(AA), an initial weight loss of 5.5% was observed, which may have been caused by the loss of unbound and bound water molecules trapped inside the matrix. Initially, the crosslinked hydrogel network was broken down into small fragments during the first step of decomposition [47]. Decarboxylation caused a weight loss of 27.55% in the first stage, which began at 230 °C. A weight loss of up to 16.93% was observed in the second stage of decomposition, which began at 370 °C. Due to depolymerization and the creation of cyclic aromatic molecules, the third stage got underway at 500 °C with a 17.22% weight loss [52, 53].

In the case of gum GgG, weight loss was observed in three stages. In the first stage, 5.5% weight loss was observed. The sample had undergone a mild dehydration stage, loss of some water molecules, and depolymerization reactions during the second stage of decomposition. The first step of

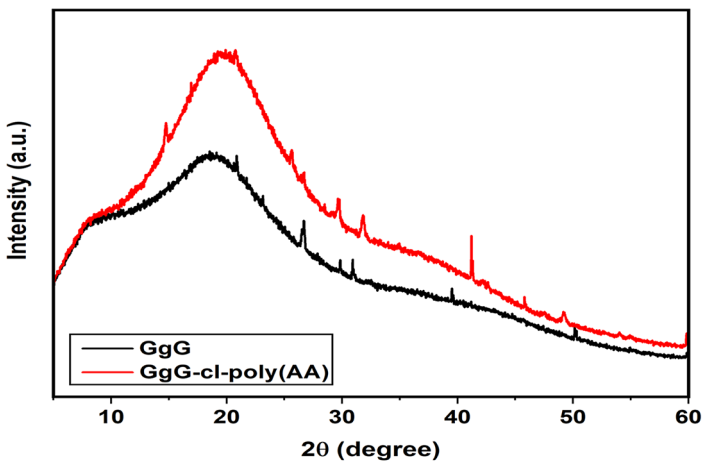

Fig. 3 XRD pattern for GgG and GgG-cl-poly(AA)

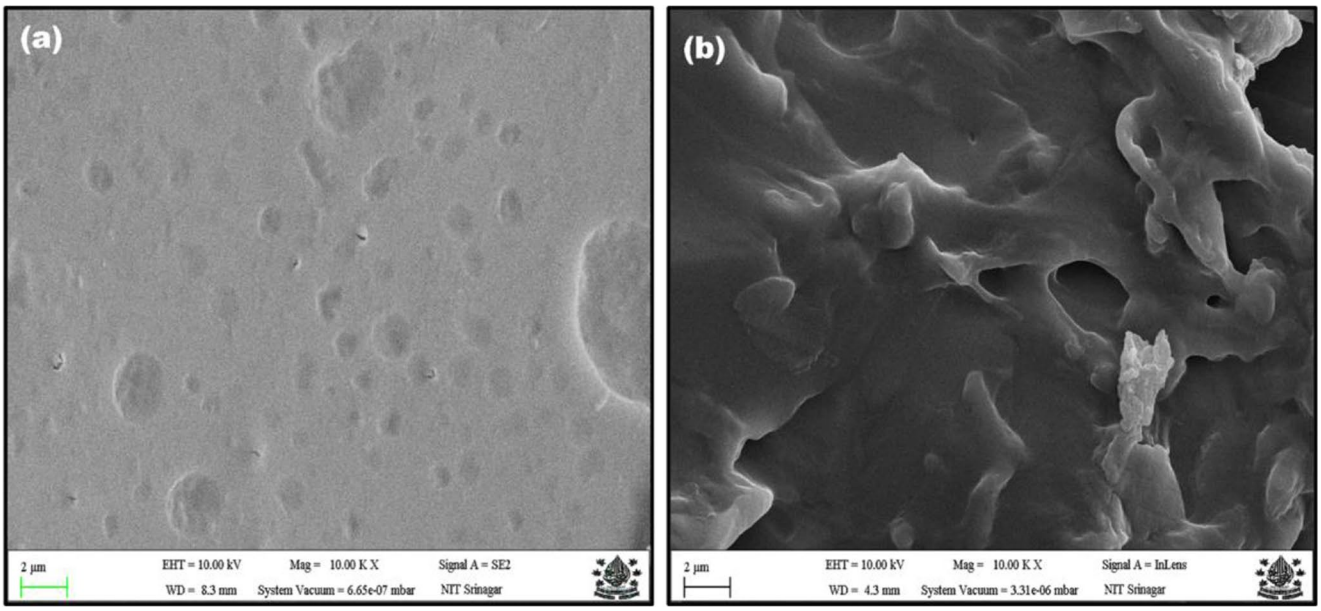

Fig. 4 SEM images of (**a**) GgG (**b**) GgG-cl-poly(AA)

Fig. 5 TGA of GgG and GgG-cl-poly(AA) hydrogel

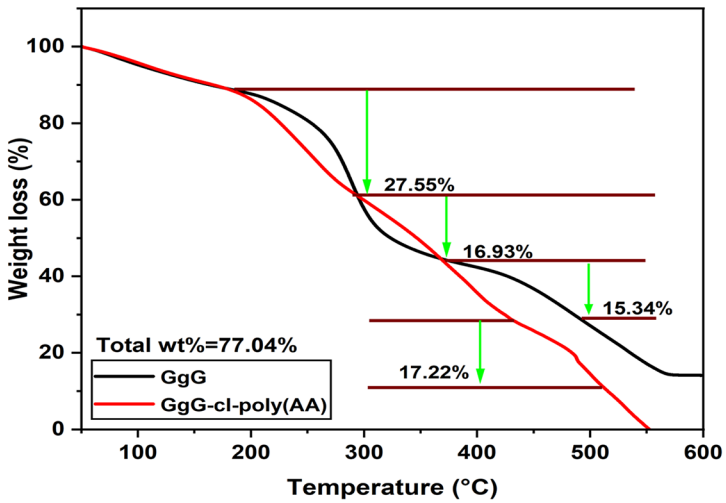

decomposition was seen between 200 and 390 °C, resulting in a weight loss of 44.48%, while the second stage occurred between 390 and 570 °C, resulting in a weight loss of 32.56% [47, 51].

3.6 ^{1}H-NMR analysis

Figure 6a depicts the ^{1}H NMR spectrum of the backbone. The broad peak at 3.3 ppm represents the characteristic feature of polysaccharides. The H-6 (methyl groups) of the converged and α and β anomers of L-rhamnopyranosyl residues are expected to be responsible for the peak at 1.30 ppm. Peaks at 2.18 ppm and 2.16 ppm are assigned to the methyl protons of the acetyl groups, while the peak ranging from 4.12 ppm and 5.12 ppm is associated with 2-acetylated D-glucopyranosyl, D-glucopyranosyl, and D-glucuropyranosyl residues [53, 54]. The peak of the aromatic proton is confirmed at 9.23 ppm [55].

Additionally, the presence of O-CH_3 groups in the gum is responsible for the peaks in the 3.1–3.9 ppm range [56]. The existence of the -CH- group of glucose is confirmed by the peak at 4.70 ppm, and the appearance of a single bond of glucuronic acid (-CH) at 5.07 ppm is consistent with records in the literature [47]. The two peaks at 2.51 ppm and 3.31 ppm are caused by protons in DMSO and a small amount of moisture. ^{1}H NMR spectrum of GgG-cl-poly(AA) shows peaks in the range of 4.95–5.99 ppm and 6.00–7.00 ppm (Fig. 6b). The monomer grafting into the hydrogel is confirmed by the ^{1}H NMR signal at 6.55 ppm, which matches the terminal COOH protons provided by the AA moieties.

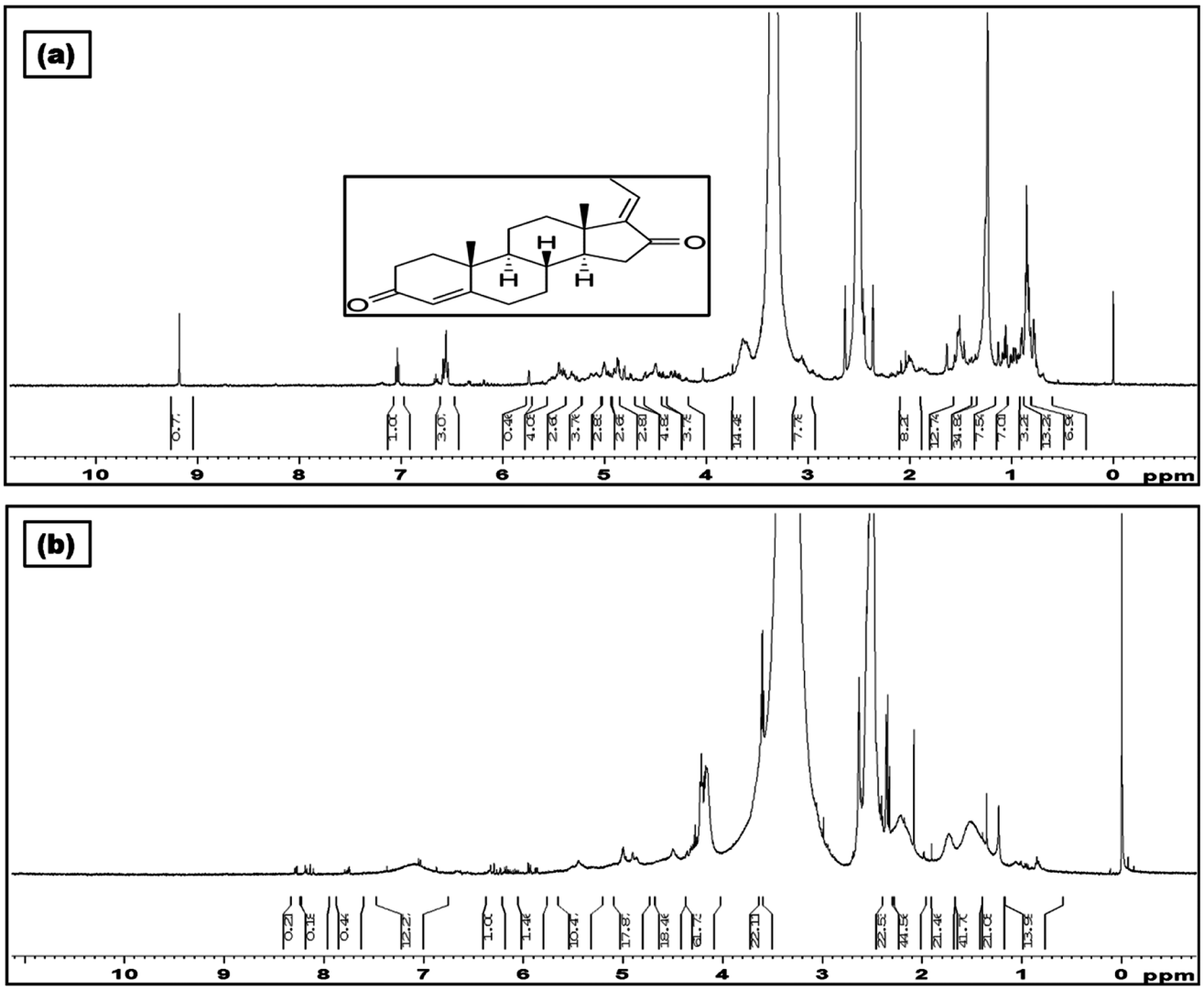

Fig. 6 ^{1}H NMR spectra of (**a**) GgG and (**b**) GgG-cl-poly(AA)

Furthermore, the N-H bond of MBA produces a strong peak of around 7.05 ppm, verifying the crosslinking of the hydrogel matrix [42].

3.7 Water retention studies in different soil samples

The amount of water available for planting or cropping depends on the water retained in different soil areas. Recent advances in agriculture, soil improvement, and crop development have increased the use of cross-linked hydrogels [57]. These hydrogel networks have a large capacity for water absorption, which enhances the soil's ability to retain water and support optimal plant growth, especially in drought-like conditions [42]. In this context, the water retention qualities of the synthesized hydrogel in different soil samples were tested by checking the weight of the samples daily until consistent results were obtained. Figure 7 shows the results of the water evaporation rate of GgG-cl-poly(AA) hydrogels. According to the experimental findings, soil samples containing hydrogel evaporated water slower than the control samples. As depicted in the graph, the water content of the different soil samples decreased over time, but the rate of water loss varied depending on whether the soil sample contained hydrogels [42]. Clay soil containing hydrogel exhibited a slower water evaporation rate than the control sample, as seen in Fig. 7a. The control sample retained the moisture level in the soil for only 10–13 days, whereas the clay soil with hydrogel could retain water for 20 days. In Fig. 7b, the control mixture evaporated entirely in 10 days, whereas the clayey and sandy soil mixture with absorbent retained water for 19 days. Figure 7c clarifies that the sandy soil with the absorbent preserved water for 18 days. The pictorial presentation of the water retention studies is shown in Fig. 7d. According to some experts, the increased water-holding

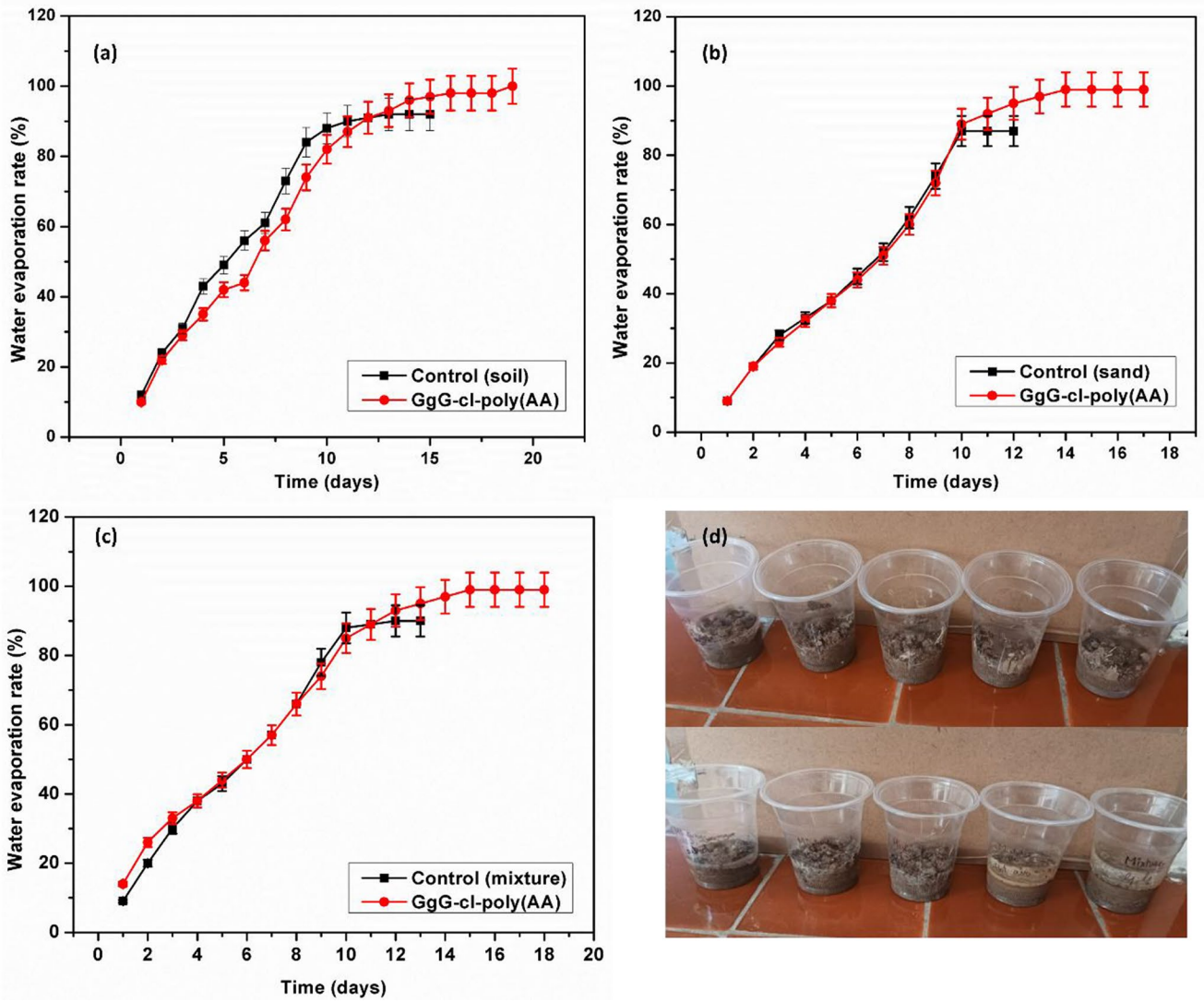

Fig. 7 Water retention studies of GgG-cl-poly(AA) in (**a**) clay soil, (**b**) sandy soil, (**c**) a mixture of sand and clay, and (**d**) test vessels containing soil, sand, and a mixture of both

capacity of hydrogels has led to an increased need for irrigation and resolved many issues related to agriculture outputs [58, 59]. Additionally, the proposed absorbent can serve as an effective soil moisture retention agent, releasing water molecules gradually for agricultural and horticultural purposes [60].

3.8 Water absorption study of GgG-cl-poly(AA) in open-air

The results of the water absorbance of GgG-cl-poly(AA) indicated a higher water retention capability (WRC). The WRC of this hydrogel at pH = 7 and 50% relative humidity is shown in Fig. 8. The GgG-cl-poly(AA) swollen hydrogel with various swelling ratios (1201, 1191, and 931) was found to sustain water content for three days even after exposure to the air at 30 °C and humidity levels around 50%. The sample exhibited a linear water loss for up to 3 days, after which it stabilized. The hydrogel's unique cross-linked structure and the multiple hydrophilic groups on the molecular chains were responsible for its exceptional water absorption in open air [44, 60].

Additionally, the water absorbed by the hydrogel might be released more readily as the temperature rises. The interaction of van der Waals forces and hydrogen bonding between the water molecules and the hydrogels determine the water retention properties [40, 47]. The exceptional qualities of the synthesized hydrogel could be helpful in agricultural applications to retain moisture and deliver nutrients to plants.

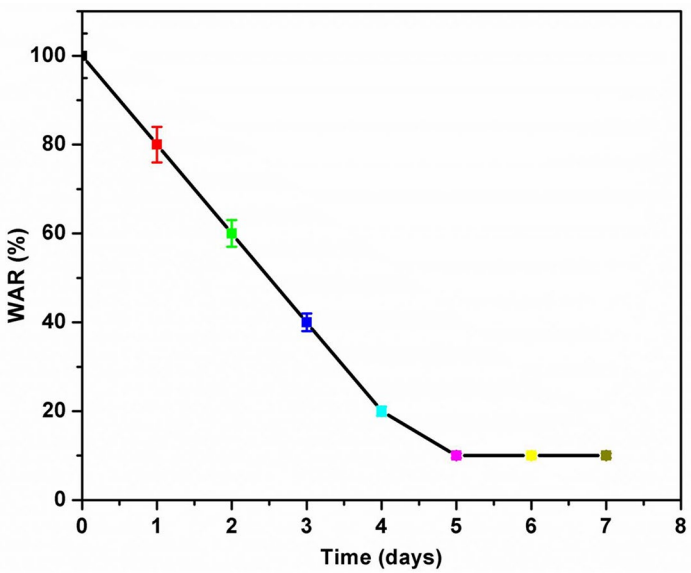

Fig. 8 Water absorption curve of GgG-cl-poly(AA) in open air

3.9 Salt resistive swelling study of GgG-cl-poly(AA) hydrogel in various salt solutions

Evaluation of the salt-resistive swelling behavior of GgG-cl-poly(AA) hydrogel is critical due to its agricultural and horticultural applications, especially for the sustained release of biofertilizers [42]. GgG-cl-poly(AA) exhibited more significant shrinking as the ionic charge increased, and the ionic species strongly influenced the swelling ratio. The swelling capacity of all hydrogel samples in NaCl, $CaCl_2$, and $FeCl_3$ solutions tends to decrease as the salt content increases, represented in Fig. 9. This decrease can be attributed to the ionic interactions between the mobile and fixed-charged ions, significantly increasing the osmotic pressure between the internal hydrogel and the external solution. These interactions help to predict hydrogels' swelling and shrinking behavior in salt solutions [35]. The swelling ratio of GgG-cl-poly(AA) dramatically decreases as the salt concentration of the solution increases [35, 61].

Additionally, the charge density on the GgG-cl-poly(AA) caused them to shrink in distinct ways depending on the chemical composition of the hydrogel network [42]. This result demonstrates that the swelling rate of hydrogels in salt solution depends on the ionic charge and salt concentration [60, 62]. The GgG-cl-poly(AA) hydrogel began to contract upon increasing the Na^+ ion concentration, possibly due to the drop in Donnan's osmotic pressure. However, it is essential to note that the swelling rate of the hydrogel sample varied depending on the specific salt solution [63]. Notably, the NaCl solution had the highest swelling ratio, followed by $CaCl_2$, while $FeCl_3$ had the lowest. Consequently, the hydrogel demonstrated intelligent swelling behavior in NaCl, $CaCl_2$, and $FeCl_3$ solutions.

3.10 Effect of the temperature on swelling percentage

The impact of temperature on the swelling percentage of the candidate polymer was examined at various temperatures (3 °C, 25 °C, 60 °C, and 80 °C) over a predetermined period of 3–4 h) as shown in Fig. 10. The hydrogel's swelling capacity varies with temperature variation, indicating that it is sensitive to warm and cold conditions [62, 64]. The swelling rate of the hydrogel increases as the temperature increases from 3 °C to 25 °C because the hydrophilic group (-COOH, $-NH_2$) establishes an intermolecular hydrogen bond with water molecules, and absorption increases rapidly [64]. A sudden increase in swelling was observed at high temperatures, which may be due to the abrupt increase in entropy and internal energy, and it further increases the diffusion of water molecules and enhances the swelling percentage [47]. The interaction among the polymeric chains and water molecules causes hydrogels to swell in water, further expanding the polymer's network structure. As the temperature rises, it disrupts the hydrogen bonding and entanglement of interconnected polymeric chains. As a result, the swelling rate increases [65, 66]. After increasing the swelling temperature from 60 °C to 80 °C, the gel expands and shows excellent water retention ability. Initially, the swelling degree increased as the swelling temperature increased, reaching its maximum value at 80 °C. This increase may be attributed to the excellent elasticity of the polymeric matrix at higher temperatures, leading to an increased swelling percentage [67, 68].

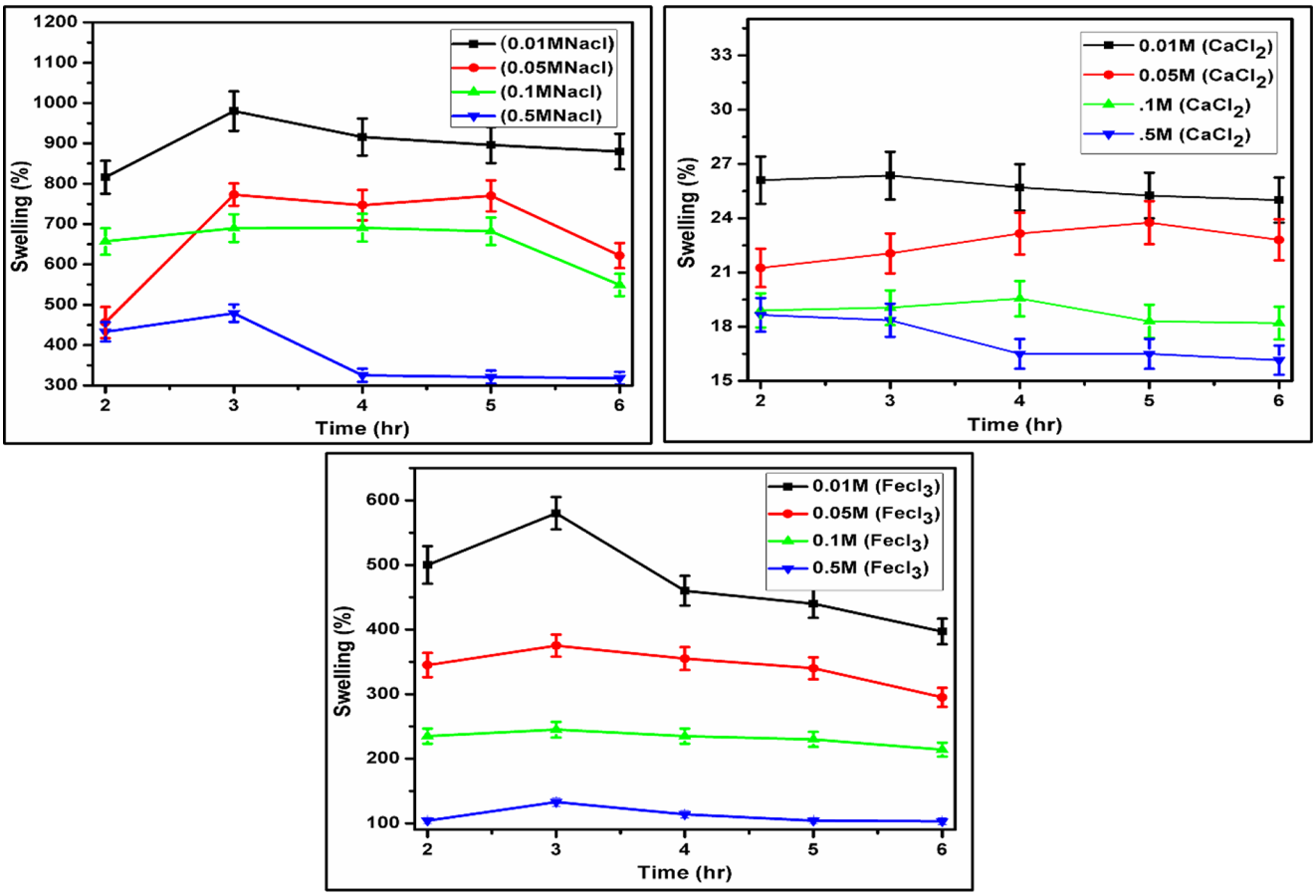

Fig. 9 Effect of different salt solutions on the swelling percentage of GgG-cl-poly(AA)

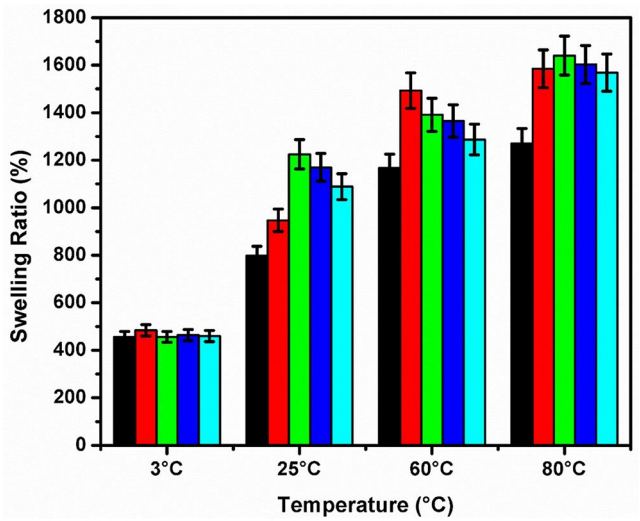

Fig. 10 Variation of swelling ratio with temperatures

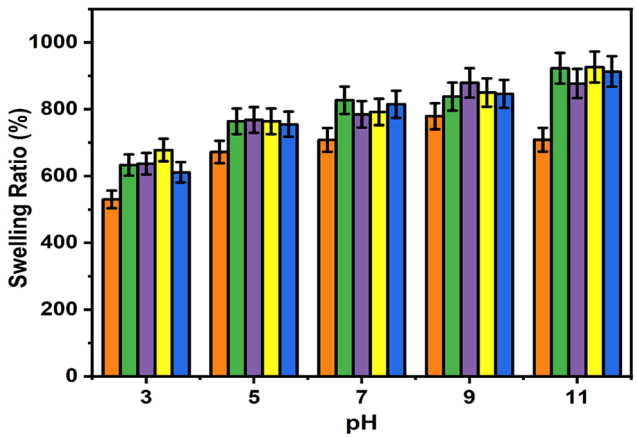

Fig. 11 Variation of swelling ratio with pH values

3.11 Effect of pH on the swelling percentage of GgG-cl-poly(AA)

Swelling studies of GgG-cl-poly(AA) were conducted at different pH levels (3.0–11.0) at a preoptimized time interval of 4 h, as shown in Fig. 11. The maximum swelling percentage (923%) was observed at pH 11, and a minimum swelling percentage (633%) was recorded in an acidic medium of pH 3. Protonation and deprotonation of COO- and COOH groups on the polymer chains were responsible for the abrupt changes in swelling behavior at different pH levels [40]. In the pH range of 3–5, the effects of extra counterions

such as Cl^- and Na^+ may be present during screening. This effect causes an extreme reduction in swelling. In highly acidic conditions, Cl^- anions may show a screening effect with (NH_3^+) ions, further preventing the effective NH_3^+-NH_3^+ ions repulsions and reducing the overall swelling percentage [62, 64]. The external pH environment significantly influences the swelling behavior of the synthesized hydrogel. Most acidic and basic functional groups are non-ionizable in the pH range of 6 to 8. Therefore, the amine and carboxylic acid may result in the cross-linking of polymer chains, further showing a reduced swelling percentage [40, 64]. In addition, a further increase in pH ionizes the carboxylic acid groups. It causes a significant increase in swelling due to electrostatic repulsions operating between the COO^- groups. However, as the pH rises above 9.0, the counter-ions (Na^+) show a screening effect that prevents the further swelling of hydrogels [66, 69]. The observed swelling pattern of GgG-cl-poly(AA) hydrogel follows the following order: pH 11 > pH9 > pH7 > pH5 > pH3.

3.12 Reswelling behaviour of GgG-cl-poly(AA) hydrogel

The ability of any hydrogel to hold and absorb water is the most crucial parameter, particularly in the agricultural field [37, 69]. The reswelling capability of GgG-cl-Poly(AA) hydrogel in distilled water following five successive swelling/drying cycles is demonstrated in Fig. 12. The breaking of polymer networks occurs due to the heavyweight and more significant pressure produced inside the hydrogel system by the absorption of water molecules [47]. Consequently, the swelling capability gradually decreases due to the closing of space between hydrogel structures with increased reswelling cycles. This is because the repeated process of swelling-deswelling breaks the physical cross-linking points of synthesized hydrogel networks and damages the crosslinked network structure [35]. As a result, both the equilibrium water absorbency and the hydrogel's capacity to store water gradually decrease. Even after five consecutive cycles of swelling and drying, the GgG-cl-poly(AA) hydrogel samples can retain a significant amount of water, with a retention percentage of 505% in distilled water. This represents only a 16.25% reduction in swelling percentage from the initial absorbing capacity of GgG-cl-poly(AA) hydrogel. These results indicate that the synthesized hydrogel sample showed a maximum swelling capacity even after multiple uses. Consequently, the generated GgG-cl-poly(AA) sample may find applications as a recyclable and reusable material in various fields [37, 47].

3.13 Biodegradation studies

Most hydrogels possess low soil degradability, and accumulating such materials in the soil causes soil pollution in the surrounding environment; hence, they are unsuitable for widespread agricultural applications [70, 71]. In the presented research work, the synthesized hydrogel based on natural gum GgG and polyacrylic acid was analyzed for biodegradation studies using two different methods, i.e., the soil burial method using garden soil and composting using vermicompost. After 65 days of analysis, the degradation pattern was observed in three distinct stages. The decomposition of polymers depends on various factors such as temperature, pH, oxygen supply, humidity, and mineral and nutrient availability, and all of these play a crucial role in the growth of microorganisms and the degradation of samples

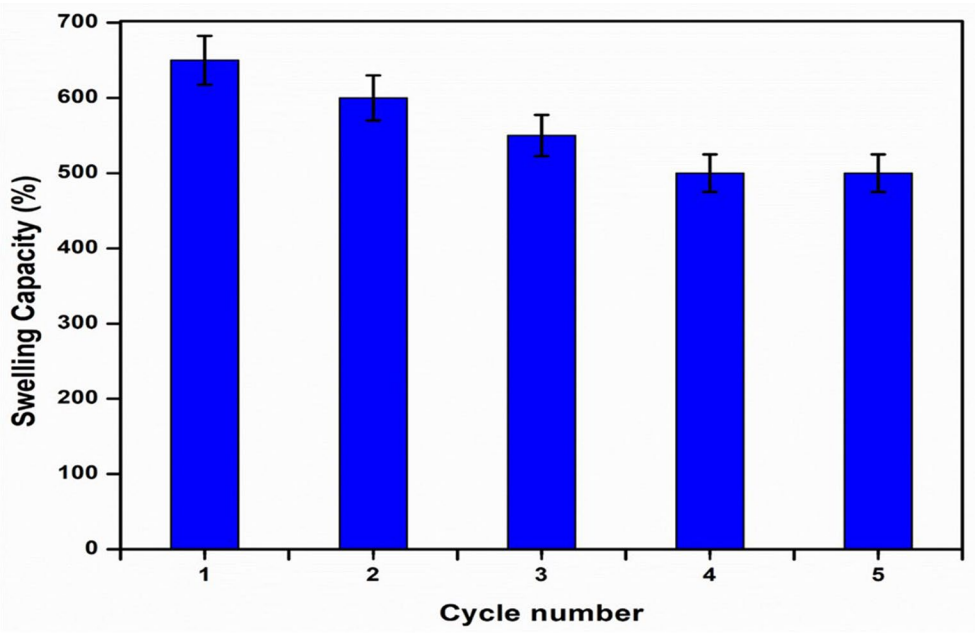

Fig. 12 Reswelling capability of GgG-cl-poly(AA) hydrogels during successive swelling/drying cycles

[72, 73]. Figure 13 shows the schematic representation and mechanism of biodegradation. Initially, we studied the impact of biodegradation after seven days in stage I of biodegradation, and this was followed by stage II after 30 days. Finally, the third stage of degradation was analyzed after 60 days [70]. This GgG-cl-poly(AA) hydrogel degradation pattern can be explained based on swelling when exposed to the soil solution. This allowed the water molecules to permeate deep inside the hydrogel's network, destroying the inner crosslinked matrix. Overall, the network architecture of the hydrogel begins to change and collapse, leading to a decreased crosslink density within the network [33].

This behavior can be attributed to the more hydrophilic character of the hydrogel matrix, which increases its hygroscopic properties, promotes the development of microorganisms during degradation, and finally degrades the crosslinked structure [34, 42]. Figure 14 depicts the degradation behavior of GgG and GgG-cl-poly(AA) hydrogels. In each case, five samples of the GgG backbone and GgG-cl-poly(AA) hydrogel were arranged in garden soil and vermicompost pots. After seven days, the samples were removed one by one, washed thoroughly, and dried in a hot air oven at 60 °C until the weight of the samples became constant. The biodegradation percentage (BD) was determined using Eq. 5. It was found that the backbone was degraded up to 82.52% through the soil burial method and 95% through the vermicomposting method of degradation.

Similarly, the final degradation percentage of GgG-cl-poly(AA) hydrogel was 85.36% and 98.21% through soil burial and vermicomposting methods, respectively. This is confirmed by Fig. 14(a-b), which proves that the degradation rate was slower in the initial stages and then increased with time. This was due to the hardness of the outer surface of dried samples, which made it more difficult for the

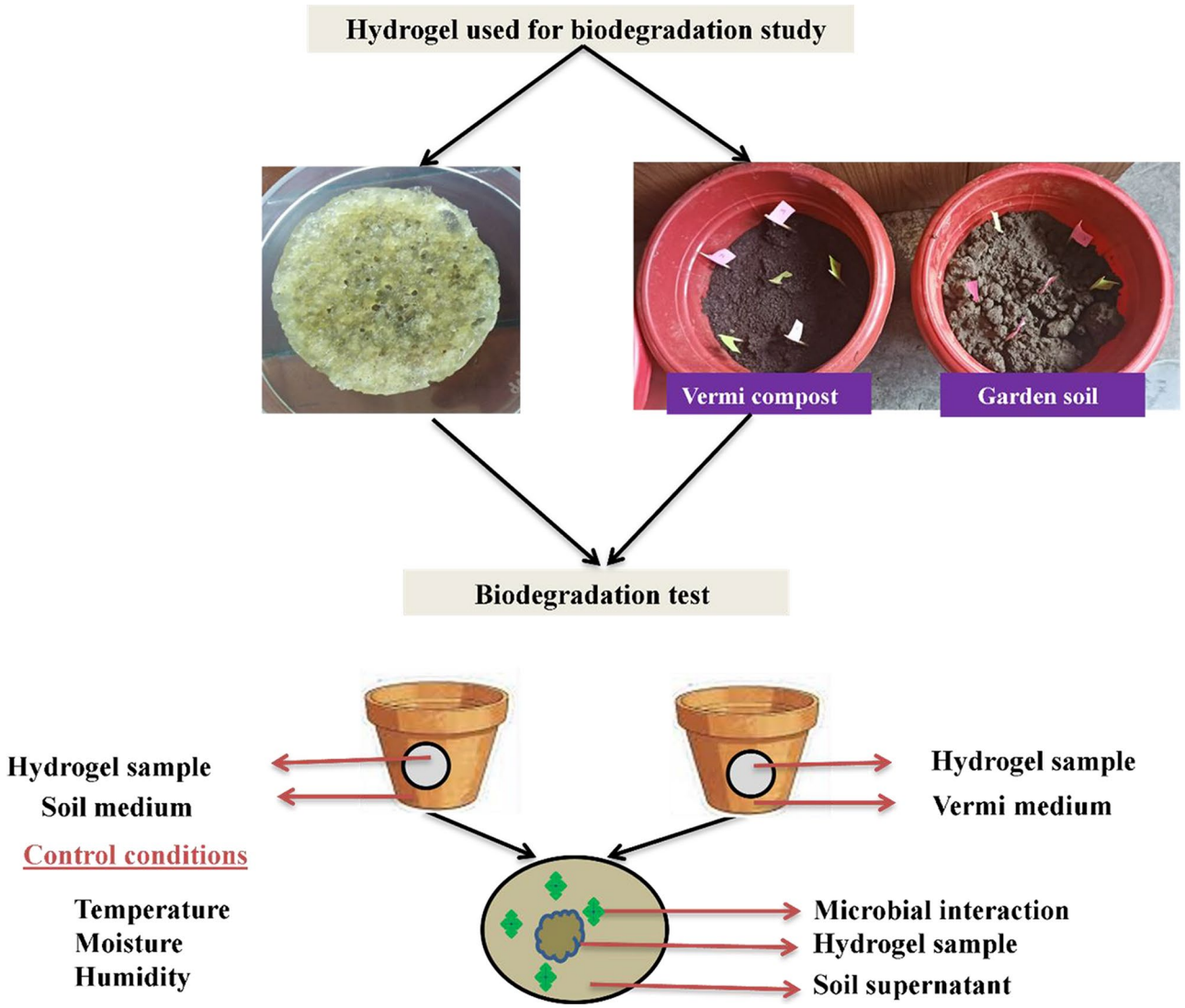

Fig. 13 Schematic presentation and mechanism of biodegradation through GgG-cl-poly(AA) hydrogel

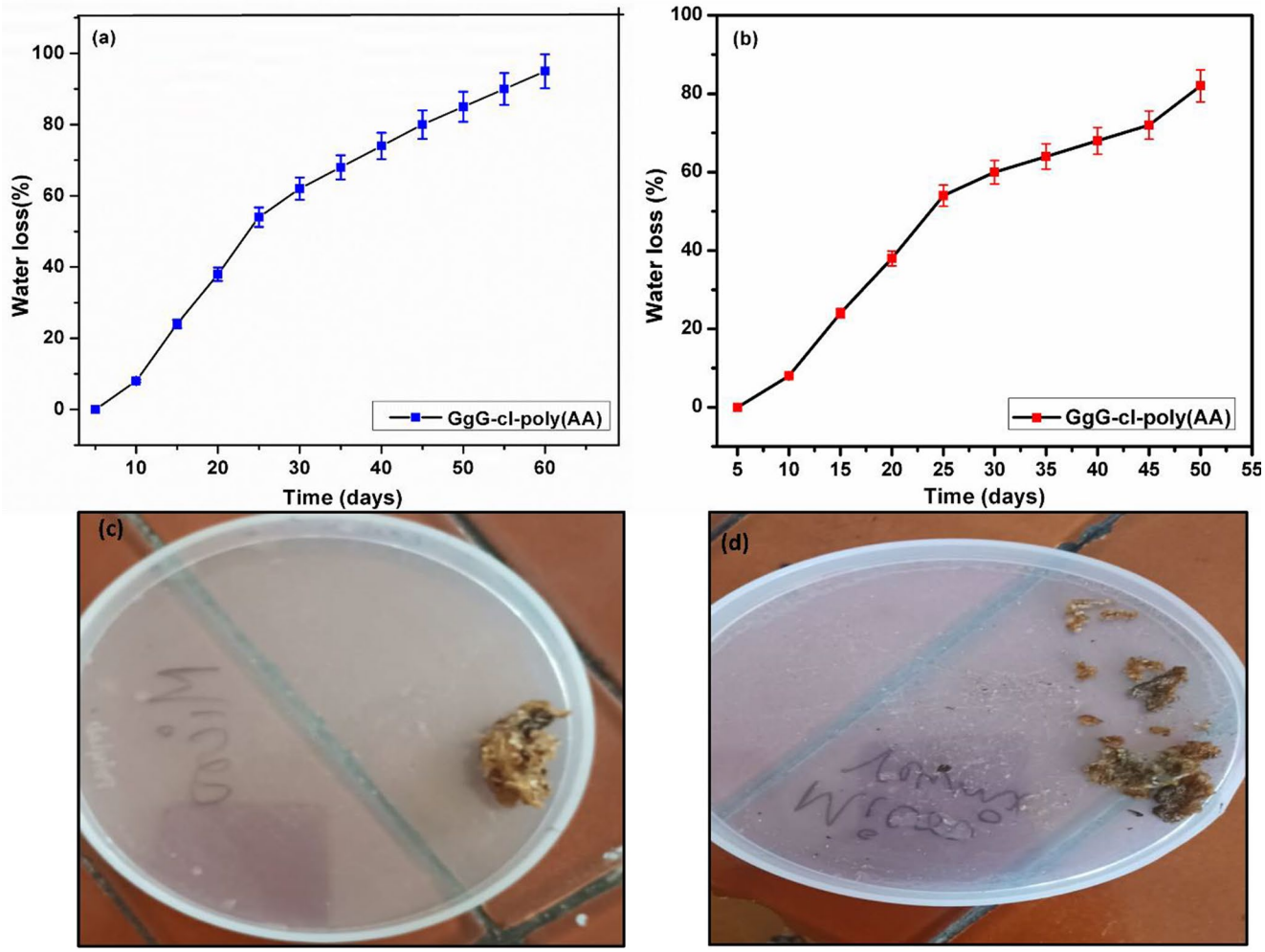

Fig. 14 Biodegradation studies of GgG-cl-poly(AA) using (**a**) soil burial and (**b**) vermicomposting method; photographs of degraded GgG-cl-poly(AA) hydrogel through (**c**) soil burial method and (**d**) vermicomposting method

enzymes to erode them earlier. Moisture played a crucial role in softening the samples, causing them to swell and triggering the growth and activity of enzymes [4]. SEM and FTIR results confirmed the breaking of bonds and loss of functional groups due to biodegradation [34, 74].

3.14 Evidence of biodegradation

According to the FTIR data, it is evident that GgG-cl-poly(AA) hydrogel begins to break down in soil and vermicompost due to bacterial indigestion and bond breaking, as depicted in Fig. 15a and b. As per FTIR data, the crosslinked network of GgG-cl-poly(AA) hydrogel in soil and vermicompost leads to breaking covalent bonds and shifting peak positions [31, 73, 75]. The distinct FTIR peaks were observed with no variation in peak strength in stage I of both biodegradation studies. However, in stage II, a notable reduction in peak intensity was observed for each functional group. This reduction may be attributed to the breakdown of bonds due to enzymatic degradation, resulting in the depolymerization of the hydrogel matrix. Eventually, the residues are absorbed by enzymes, which metabolize them into carbon dioxide and other gases. Stage III of biodegradation demonstrated enhanced polymeric chain oxidation to mineral ions and gases [4, 36, 76].

SEM analysis clearly showed the structural and morphological changes occurring on the sample's surface. As the biodegradation time increases, the morphological damage becomes more severe, as seen in the picture of SEM in Fig. 16a, b, c, d, and e. Due to the breakdown of the crosslinked hydrogel matrix, various types of small gaps, fractures, and cracks were observed on the surface of GgG and GgG-cl-poly(AA) through both soil burial and vermicomposting methods [11]. SEM images of GgG depicted a cloudy morphology due to complete alteration by enzymes, represented in Fig. 16a.

The SEM images of degraded GgG-cl-poly(AA) hydrogels obtained through vermicomposting and soil burial

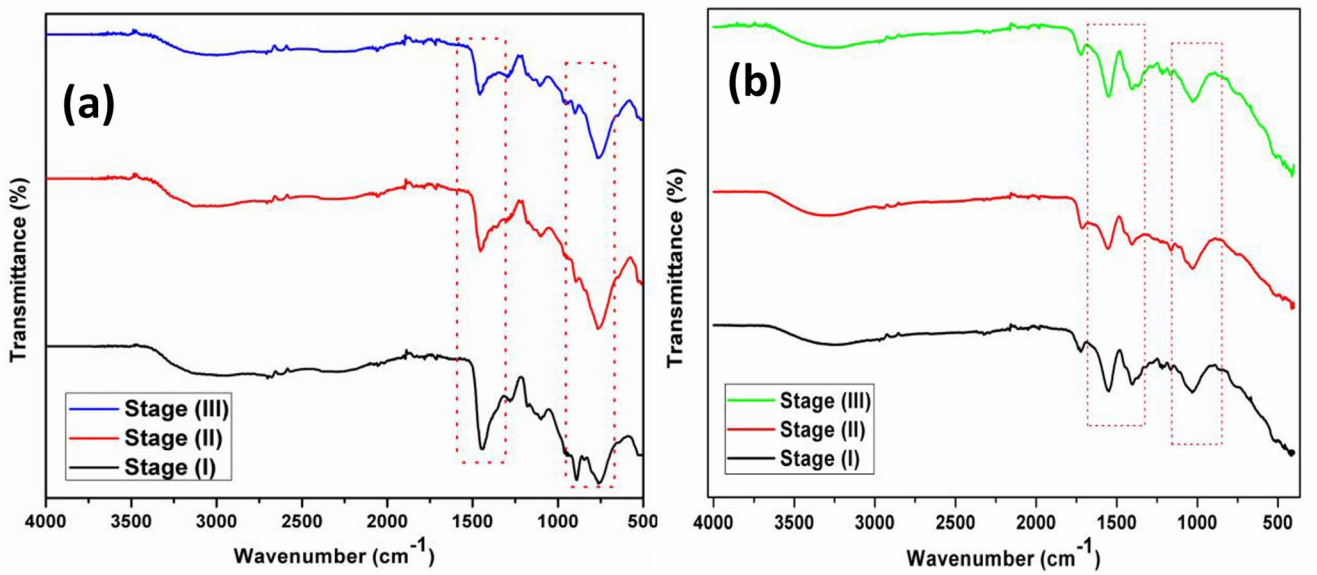

Fig. 15 FTIR spectra of degraded GgG-cl-poly(AA) hydrogel (**a**) soil burial method, and (**b**) vermicomposting method

methods exhibit minor visible changes consistent with the earlier degradation rates and show surface pits and cracks seen in Fig. 16b and d. Crosslinks were found to disappear as the surface eroded due to enzymatic action, making the structure opaque. Enzymatic secretion and microbial attack during the vermicomposting process enhance the hydrogel porosity, size, brittleness, and number of cracks, leading to increased heterogeneity and irregularity [42]. Figure 16c, e shows a completely porous and fractured structure. The complete breakdown of covalent connections between various polymeric chains due to chemical and enzymatic degradation is likely the source of accelerated degradation at this stage [11, 12, 42].

In conclusion, the morphological analysis indicated that both soil burial and vermicomposting tests result in the degradation of the GgG and GgG-cl-poly(AA) crosslinked networks. The degradation process demonstrates that GgG-cl-poly(AA) hydrogel has no detrimental effects on soil fertility. Instead, it enhances the organic matter content in the soil and accelerates water retention, leading to improved crop yield [69].

4 Conclusion

In this study, we synthesized GgG-cl-poly(AA) hydrogel using a microwave synthesis method with AA as a monomer, APS as an initiator, and MBA as a crosslinking agent, resulting in good swelling and water-retaining properties. This approach is practical, quick, effective, and cost-effective for producing natural hydrogels. The synthesized samples were optimized to achieve a maximum swelling percentage. The water retention capability demonstrated that the prepared hydrogel takes 22 days to evaporate completely. Moreover, the moisture release ratio was over 60% even after three days of exposure to open air at ambient temperature. The synthesized hydrogel exhibited substantial swelling under different temperature and pH conditions. This research also reveals that the prepared hydrogel possesses reswelling ability with only a 16.78% loss after five repetitions.

Furthermore, biodegradation experiments indicated that vermicompost soil degraded hydrogels faster than garden soil. GgG-cl-poly(AA) hydrogel exhibited a lower swelling in different salt solution concentrations than aqueous solutions. Consequently, the synthesized GgG-cl-poly(AA) hydrogel can be utilized in agricultural applications as a soil conditioner and a water-conserving agent. Additionally, these polymers can serve as carriers for transporting nutrients in agrarian fields.

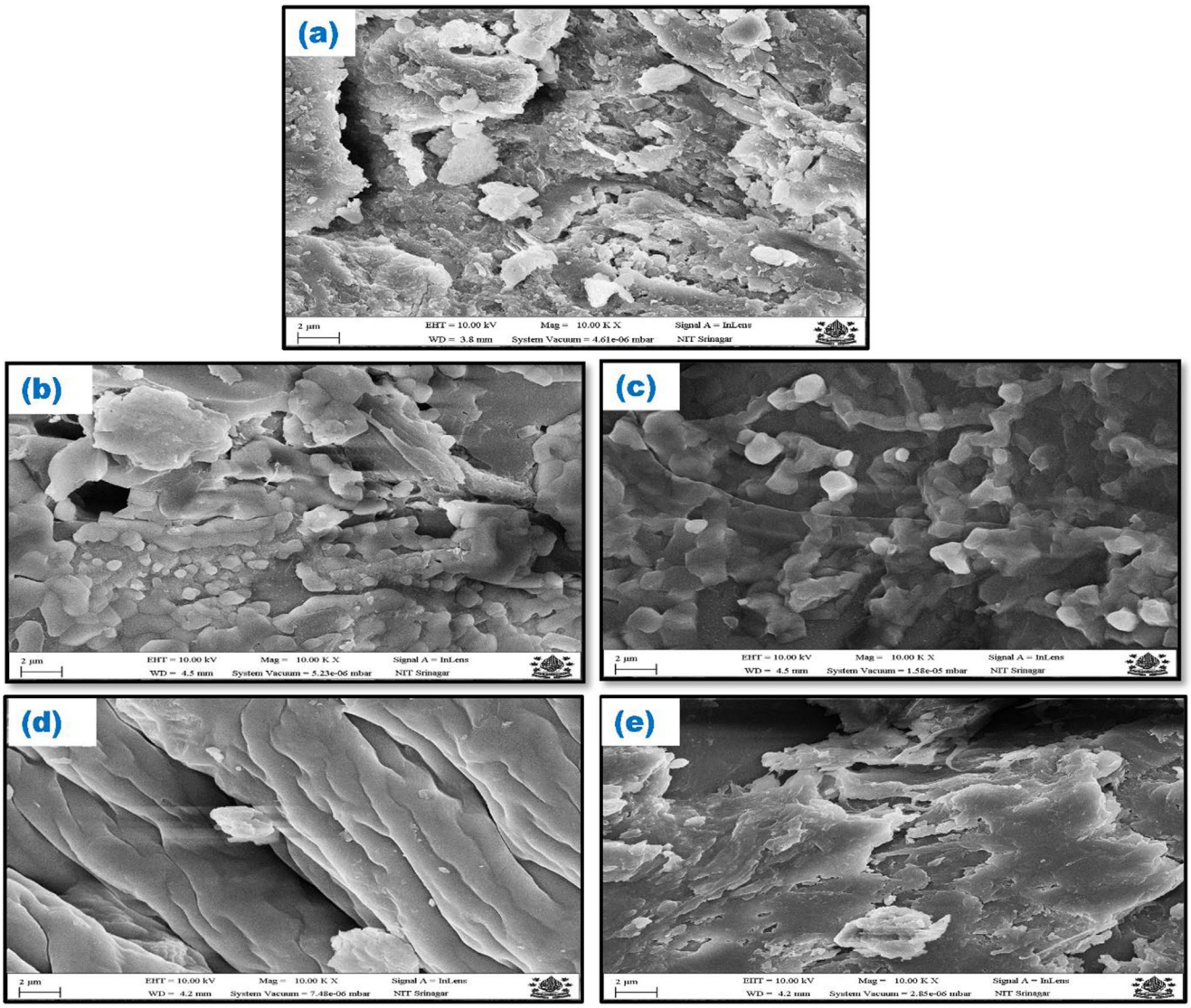

Fig. 16 SEM image of degraded (**a**) GgG backbone; (**b**) GgG-cl-poly(AA) hydrogel through the vermicomposting method in the initial stage of decomposition and (**c**) final stage of decomposition; (**d**) initial stage of decomposition and (**e**) final stage of decomposition

Author contributions Shabnum Saleem: Methodology, synthesis, characterization, writing – original draft; Kashma Sharma: Conceptualization, Investigation, Data curation, editing, Supervision; Amit Kumar Sharma: Investigation, Data curation, editing; Vishal Sharma: Visualization, Reviewing and Editing; Vaneet Kumar: Supervision, Writing- Reviewing and Editing, project administration; Vijay Kumar: Validation, Supervision, Writing- Reviewing and Editing, project administration.

Funding This work was supported by IIT Ropar Technology and Innovation Foundation for Agriculture and Water Technology Development Hub (AWaDH) (File Number: AWaDH-SpINe/IITRPR/2022/P10005/02).

Data availability No datasets were generated or analysed during the current study.

Declarations

Ethical approval Not applicable.

Competing interests The authors declare no competing interests.

References

1. Raziq, A., de Verdier, K., Younas, M.: Rapid change of strategy is necessary for developing dromedary camel pastoralism in the Cholistan desert of Pakistan. Pastoralism: Res. Policy Pract. **1**(1), 1–9 (2011)
2. Cloutier, S., McCallum, B.D., Loutre, C., Banks, T.W., Wicker, T., Feuillet, C., Jordan, M.C.: Leaf rust resistance gene Lr1, isolated from bread wheat (Triticum aestivum L.) is a member of the large psr567 gene family. Plant Mol. Biol. **65**(1), 93–106 (2007)
3. Xiong, W., Conway, D., Xu, Y.L., Jinhe, J., Ju, H., Calsamigliamendlewicz, S., et al.: The Impacts of Climate Change on

Chinese agriculture - phase Ii National Level Study Final Report. Aea Group UK (2008)
4. Liu, C., Lei, F., Li, P., Jiang, J., Wang, K.: Borax crosslinked fenugreek galactomannan hydrogel as potential water-retaining agent in agriculture. Carbohydr. Polym. **236**, 116100 (2020)
5. Han, B., Benner, S.G., Flores, A.N.: Evaluating impacts of climate change on future water scarcity in an intensively managed semi-arid region using a coupled model of biophysical processes and water rights. Hydrol. Earth Syst. Sci. Dis., 1–53 (2018)
6. Fan, T., Stewart, B.A., Payne, W.A., Yong, W., Luo, J., Gao, Y.: Long-term fertilizer and water availability effects on cereal yield and soil chemical properties in northwest China. Soil Sci. Soc. Am. J. **69**(3), 842–855 (2005)
7. Wei, Y., Durian, D.J.: Rain water transport and storage in a model sandy soil with hydrogel particle additives. Eur. Phys. J. E. **37**(10), 1–11 (2014)
8. Eko, R.M., Laguë, C.: Influence of structure on the mechanical behavior of an agricultural clay soil. Agricultural Eng. International: CIGR J. **14**(4), 1–8 (2012)
9. Deshmukh, G., Hardaha, M.K.: Effect of irrigation and fertigation scheduling under drip irrigation in papaya. J. AgriSearch, **1**(4). (2014)
10. Alcamo, J., Henrichs, T., Rosch, T.: World water in 2025. *World Water Series Report*, *2* (2000)
11. Tiwari, R., Krishnamoorthi, S., Kumar, K.: Synthesis of crosslinker devoid novel hydrogels: Swelling behaviour and controlled urea release studies. J. Environ. Chem. Eng. **7**(4), 103162 (2019)
12. Al-Jabari, M., Ghyadah, R.A., Alokely, R.: Recovery of hydrogel from baby diaper wastes and its application for enhancing soil irrigation management. J. Environ. Manage. **239**, 255–261 (2019)
13. Sayed, A., Mohamed, M.M., Abdel-raouf, M.E.S., Mahmoud, G.A.: Radiation synthesis of green nanoarchitectonics of guar gum-pectin/polyacrylamide/zinc oxide superabsorbent hydrogel for sustainable agriculture. J. Inorg. Organomet. Polym Mater. **32**(12), 4589–4600 (2022)
14. Panigrahi, P., Sahu, N.N., Pradhan, S.: Evaluating partial root-zone irrigation and mulching in okra (Abelmoschus esculentus L.) under a sub-humid tropical climate. J. Agric. Rural Dev. Tropics Subtropics (JARTS). **112**(2), 169–175 (2011)
15. Brahma, S., Phookan, D.B., Kachari, M., Hazarika, T.K., Das, K.: Growth, yield and economics of broccoli under different levels of nitrogen fertigation. Indian J. Hortic. **67**(4), 279–282 (2010)
16. Abd El-Wahed, M.H., Ali, E.A.: Effect of irrigation systems, amounts of irrigation water and mulching on corn yield, water use efficiency and net profit. Agric. Water Manage. **120**, 64–71 (2013)
17. Keivanfar, S., Fotouhi Ghazvini, R., Ghasemnezhad, M., Mousavi, A., Khaledian, M.R.: Effects of regulated deficit irrigation and superabsorbent polymer on fruit yield and quality of'granny smith'apple. Agriculturae Conspectus Scientificus. **84**(4), 383–389 (2019)
18. Mittal, H., Al Alili, A., Morajkar, P.P., Alhassan, S.M.: Crosslinked hydrogels of polyethylenimine and graphene oxide to treat cr (VI) contaminated wastewater. Colloids Surf., a. **630**, 127533 (2021)
19. Mittal, H., Alili, A., A., Alhassan, S.M.: Hybrid super-porous hydrogel composites with high water vapor adsorption capacity–adsorption isotherm and kinetics studies. J. Environ. Chem. Eng. **9**(6), 106611 (2021)
20. Dehkordi, D.K., Seyyedboveir, S.: Evaluation of super AB A 200 superabsorbent on water use efficiency and yield response factor of SCKaroun701 corn under deficit irrigation. Adv. Environ. Biology, 4615–4623 (2013)
21. Bennour, S., Louzri, F.: Study of swelling properties and thermal behavior of poly (N, N-dimethylacrylamide-co-maleic acid) based hydrogels. Adv. Chem. **2014**, 1–10 (2014)
22. Gao, X., He, C., Xiao, C., Zhuang, X., Chen, X.: Biodegradable pH-responsive polyacrylic acid derivative hydrogels with tunable swelling behavior for oral delivery of insulin. Polymer. **54**(7), 1786–1793 (2013)
23. Arizaga, A., Ibarz, G., Piñol, R.: Stimuli-responsive poly (4-vinyl pyridine) hydrogel nanoparticles: Synthesis by nanoprecipitation and swelling behavior. J. Colloid Interface Sci. **348**(2), 668–672 (2010)
24. Montero-Rama, M.P., Liras, M., García, O., Quijada-Garrido, I.: Thermo-and pH-sensitive hydrogels functionalized with thiol groups. Eur. Polymer J. **63**, 37–44 (2015)
25. Xia, M., Wu, W., Liu, F., Theato, P., Zhu, M.: Swelling behavior of thermosensitive nanocomposite hydrogels composed of oligo (ethylene glycol) methacrylates and clay. Eur. Polymer J. **69**, 472–482 (2015)
26. Ahmed, E.M.: Hydrogel: Preparation, characterization, and applications: A review. J. Adv. Res. **6**(2), 105–121 (2015)
27. Yamato, M., Konno, C., Utsumi, M., Kikuchi, A., Okano, T.: Thermally responsive polymer-grafted surfaces facilitate patterned cell seeding and co-culture. Biomaterials. **23**(2), 561–567 (2002)
28. Albertsson, A.C., Voepel, J., Edlund, U., Dahlman, O., Söderqvist-Lindblad, M.: Design of renewable hydrogel release systems from fiberboard mill wastewater. Biomacromolecules. **11**(5), 1406–1411 (2010)
29. Sun, X.F., Gan, Z., Jing, Z., Wang, H., Wang, D., Jin, Y.: Adsorption of methylene blue on hemicellulose-based stimuli-responsive porous hydrogel. J. Appl. Polym. Sci., **132**(10). (2015)
30. Fathi, M., Alami-Milani, M., Geranmayeh, M.H., Barar, J., Erfan-Niya, H., Omidi, Y.: Dual thermo-and pH-sensitive injectable hydrogels of chitosan/(poly (N-isopropylacrylamide-co-itaconic acid)) for doxorubicin delivery in breast cancer. Int. J. Biol. Macromol. **128**, 957–964 (2019)
31. Kaith, B.S., Shanker, U., Gupta, B.: Synergic effect of Guggul gum based hydrogel nanocomposite: An approach towards adsorption-photocatalysis of Magenta-O. Int. J. Biol. Macromol. **161**, 457–469 (2020)
32. Mittal, H., Alili, A., A., Alhassan, S.M.: Latest progress in utilizing gum hydrogels and their composites as high-efficiency adsorbents for removing pollutants from wastewater. J. Mol. Liq., 123392. (2023)
33. Khaliq, G., Saleh, A., Bugti, G.A., Hakeem, K.R.: Guggul gum incorporated with basil essential oil improves quality and modulates cell wall-degrading enzymes of jamun fruit during storage. Sci. Hort. **273**, 109608 (2020)
34. Kaith, B.S., Shanker, U., Gupta, B.: One-pot green synthesis of polymeric nanocomposite: Biodegradation studies and application in sorption-degradation of organic pollutants. J. Environ. Manage. **234**, 345–356 (2019)
35. Ahmad, S., Manzoor, K., Purwar, R., Ikram, S.: Morphological and swelling potential evaluation of moringa oleifera gum/poly (vinyl alcohol) hydrogels as a superabsorbent. ACS Omega. **5**(29), 17955–17961 (2020)
36. Meng, Y., Liu, X., Li, C., Liu, H., Cheng, Y., Lu, J., Wang, H.: Super-swelling lignin-based biopolymer hydrogels for soil water retention from paper industry waste. Int. J. Biol. Macromol. **135**, 815–820 (2019)
37. Abdallah, A.M.: The effect of hydrogel particle size on water retention properties and availability under water stress. Int. soil. Water Conserv. Res. **7**(3), 275–285 (2019)
38. Patra, S. K., Poddar, R., Brestic, M., Acharjee, P. U., Bhattacharya, P., Sengupta,S., … Hossain, A. (2022). Prospects of hydrogels in agriculture for enhancing crop and water productivity under water deficit condition. *International Journal of Polymer Science*, *2022*

39. Iftime, M.M., Ailiesei, G.L., Ungureanu, E., Marin, L.: Designing Chitosan based eco-friendly multifunctional soil conditioner systems with urea-controlled release and water retention. Carbohydr. Polym. **223**, 115040 (2019)
40. Chen, M., Ni, Z., Shen, Y., Xiang, G., Xu, L.: Reinforced swelling and water-retention properties of super-absorbent hydrogel fabricated by a dual stretchable single network tactic. Colloids Surf., a. **602**, 125133 (2020)
41. Dave, V., Yadav, R.B., Gupta, S., Sharma, S.: Guggulosomes: A herbal approach for enhanced topical delivery of phenylbutazone. Future J. Pharm. Sci. **3**(1), 23–32 (2017)
42. Choudhary, S., Sharma, K., Bhatti, M.S., Sharma, V., Kumar, V.: DOE-based synthesis of gellan gum-acrylic acid-based biodegradable hydrogels: Screening of significant process variables and in situ field studies. RSC Adv. **12**(8), 4780–4794 (2022)
43. Chang, L., Xu, L., Liu, Y., Qiu, D.: Superabsorbent polymers used for agricultural water retention. Polym. Test. **94**, 107021 (2021)
44. Chen, T., Liu, H., Dong, C., An, Y., Liu, J., Li, J., … Zhang, M. (2020). Synthesis and characterization of temperature/pH dual sensitive hemicellulose-based hydrogels from eucalyptus APMP waste liquor. *Carbohydrate polymers*, *247*, 116717
45. Arun Krishna, K., Vishalakshi, B.: Gellan gum-based novel composite hydrogel: Evaluation as adsorbent for cationic dyes. J. Appl. Polym. Sci. **134**(47), 45527 (2017)
46. Choudhary, S., Sharma, K., Kumar, V., Bhatia, J.K., Sharma, S., Sharma, V.: Microwave-assisted synthesis of gum gellan-cl-poly (acrylic-co-methacrylic acid) hydrogel for cationic dyes removal. Polym. Bull. **77**, 4917–4935 (2020)
47. Tanan, W., Panichpakdee, J., Saengsuwan, S.: Novel biodegradable hydrogel based on natural polymers: Synthesis, characterization, swelling/reswelling and biodegradability. Eur. Polymer J. **112**, 678–687 (2019)
48. Kaith, B.S., Jindal, R., Mittal, H., Kumar, K.: Synthesis, characterization, and swelling behavior evaluation of hydrogels based on gum ghatti and acrylamide for selective absorption of saline from different petroleum fraction–saline emulsions. J. Appl. Polym. Sci. **124**(3), 2037–2047 (2012)
49. Mittal, H., Maity, A., Ray, S.S.: Gum karaya based hydrogel nanocomposites for the effective removal of cationic dyes from aqueous solutions. Appl. Surf. Sci. **364**, 917–930 (2016)
50. Cheng, D., Liu, Y., Yang, G., Zhang, A.: Water-and fertilizer-integrated hydrogel derived from the polymerization of acrylic acid and urea as a slow-release N fertilizer and water retention in agriculture. J. Agric. Food Chem. **66**(23), 5762–5769 (2018)
51. Zhang, T., Huang, J.: N-vinylimidazole modified hyper-cross-linked resins and their adsorption toward rhodamine B: Effect of the cross-linking degree. J. Taiwan Inst. Chem. Eng. **80**, 293–300 (2017)
52. El-Sayed Abdel-Raouf, M., Kamal, R.S., Hegazy, D.E., Sayed, A.: Gamma irradiation synthesis of carboxymethyl chitosan-nanoclay hydrogel for the removal of cr (VI) and pb (II) from aqueous media. J. Inorg. Organomet. Polym Mater. **33**(4), 895–913 (2023)
53. Prime, R.B., Bair, H.E., Vyazovkin, S., Gallagher, P.K., Riga, A.: Thermogravimetric analysis (TGA). *Thermal analysis of polymers: Fundamentals and applications*, 241–317 (2009)
54. Mankotia, P., Sharma, K., Sharma, V., Mishra, Y.K., Kumar, V.: Curcumin-loaded Butea monosperma gum-based hydrogel: A new excipient for controlled drug delivery and anti-bacterial applications. Int. J. Biol. Macromol. **242**, 124703 (2023)
55. Mahmoud, G.A., Sayed, A., Abdel-raouf, M.E.S., Danial, M.Y., Amin, A.: Efficient removal of cr (VI) from aqueous solutions using chitosan/Na-alginate bio-based nanocomposite hydrogel. J. Appl. Polym. Sci., **140**(21), e53886. (2023)
56. Sharma, S., Virk, K., Sharma, K., K Bose, S., Kumar, V., Sharma, V., Kalia, S.: Preparation of gum acacia-poly (acrylamide-IPN-acrylic acid) based nanocomposite hydrogels via polymerization methods for antimicrobial applications. J. Mol. Struct. **1215**, 128298 (2020)
57. Shahid, S.A., Qidwai, A.A., Anwar, F., Ullah, I., Rashid, U.: Improvement in the water retention characteristics of sandy loam soil using a newly synthesized poly (acrylamide-co-acrylic acid)/AlZnFe2O4 superabsorbent hydrogel nanocomposite material. Molecules. **17**(8), 9397–9412 (2012)
58. Zhang, Y., Zhao, L., Chen, Y.: Synthesis and characterization of starch-g-Poly (acrylic acid)/Organo-Zeolite 4 a superabsorbent composites with respect to their water-holding capacities and nutrient-release behavior. Polym. Compos. **38**(9), 1838–1848 (2017)
59. Soppimath, K.S., Aminabhavi, T.M., Kulkarni, A.R., Rudzinski, W.E.: Biodegradable polymeric nanoparticles as drug delivery devices. J. Controlled Release. **70**(1–2), 1–20 (2001)
60. Shivakumara, L.R., Demappa, T.: Synthesis and swelling behavior of sodium alginate/poly (vinyl alcohol) hydrogels. Turkish J. Pharm. Sci. **16**(3), 252 (2019)
61. Mittal, H., Alili, A., A., Alhassan, S.M.: Development of high efficacy super-porous hydrogel composites-based polymer desiccants to capture water vapors from moist air. Adsorption, 1–17. (2024)
62. Chang, C., He, M., Zhou, J., Zhang, L.: Swelling behaviors of pH-and salt-responsive cellulose-based hydrogels. Macromolecules. **44**(6), 1642–1648 (2011)
63. Wadi, V.S., Mittal, H., Fosso-Kankeu, E., Jena, K.K., Alhassan, S.M.: Mercury removal by porous sulfur copolymers: Adsorption isotherm and kinetics studies. Colloids Surf., a. **606**, 125333 (2020)
64. Bhosale, R.R., Gangadharappa, H.V., Osmani, R.A.M., Gowda, D.V.: Design and development of polymethylmethacrylate-grafted gellan gum (PMMA-g-GG)-based pH-sensitive novel drug delivery system for antidiabetic therapy. Drug Delivery Translational Res. **10**, 1002–1018 (2020)
65. Jayaramudu, T., Ko, H.U., Kim, H.C., Kim, J.W., Kim, J.: Swelling behavior of polyacrylamide–cellulose nanocrystal hydrogels: Swelling kinetics, temperature, and pH effects. *Materials*, *12*(13), 2080. (2019)
66. Zhao, Y., Su, H., Fang, L., Tan, T.: Superabsorbent hydrogels from poly (aspartic acid) with salt-, temperature-and pH-responsiveness properties. Polymer. **46**(14), 5368–5376 (2005)
67. Aboelkhir, D.M., Sayed, A., Eldondaity, L.S., Joseph, V., Amin, A., Mahmoud, G.A.: Multiwalled carbon nanotubes@ pectin/κ-carrageenan-based nanocomposite biohydrogel prepared by gamma irradiation for efficient methylene blue dye sequestration. J. Appl. Polym. Sci., **141**(22), e55452. (2024)
68. Singh, B., Sharma, V., Kumar, R., Mohan, M.: Development of dietary fiber psyllium based hydrogel for use in drug delivery applications. Food Hydrocoll. Health. **2**, 100059 (2022)
69. Li, Q., Ma, Z., Yue, Q., Gao, B., Li, W., Xu, X.: Synthesis, characterization and swelling behavior of superabsorbent wheat straw graft copolymers. Bioresour. Technol. **118**, 204–209 (2012)
70. Phetwarotai, W., Potiyaraj, P., Aht-Ong, D.: Biodegradation of polylactide and gelatinized starch blend films under controlled soil burial conditions. J. Polym. Environ. **21**, 95–107 (2013)
71. Sharma, P., Mittal, H., Jindal, R., Jindal, D., Alhassan, S.M.: Sustained delivery of atenolol drug using gum dammar crosslinked polyacrylamide and zirconium based biodegradable hydrogel composites. Colloids Surf., a. **562**, 136–145 (2019)
72. Warkar, S.G., Kumar, A.: Synthesis and assessment of carboxymethyl tamarind kernel gum based novel superabsorbent hydrogels for agricultural applications. Polymer. **182**, 121823 (2019)

73. Mittal, H., Jindal, R., Kaith, B.S., Maity, A., Ray, S.S.: Flocculation and adsorption properties of biodegradable gum-ghatti-grafted poly (acrylamide-co-methacrylic acid) hydrogels. Carbohydr. Polym. **115**, 617–628 (2015)
74. Mehta, P., Kaith, B.S.: In-situ fabrication of rod-shaped nano-hydroxyapatite using microwave assisted semi-interpenetrating network as a template-morphology controlled approach. Mater. Chem. Phys. **208**, 49–60 (2018)
75. Thombare, N., Mishra, S., Siddiqui, M.Z., Jha, U., Singh, D., Mahajan, G.R.: Design and development of guar gum based novel, superabsorbent and moisture retaining hydrogels for agricultural applications. Carbohydr. Polym. **185**, 169–178 (2018)
76. Maiti, M., Kaith, B.S., Jindal, R., Jana, A.K.: Synthesis and characterization of corn starch based green composites reinforced with Saccharum spontaneum L graft copolymers prepared under micro-wave and their effect on thermal, physio-chemical and mechanical properties. Polym. Degrad. Stab. **95**(9), 1694–1703 (2010)